UNIVERSITY OF CAMBRIDGE
Department of Engineering

CFD Simulation of the Rainfall-Runoff Processes

D-DL359-2

Author Name: Nathen Chung

Supervisor: Dr. Dongfang Liang

Date: 27th May 2020

I hereby declare that, except where specifically indicated, the work submitted herein is my own original work.

Signed ____________________ *Date* 27/05/20

Technical Abstract

This report set out to investigate the effects of roughness and macro-roughness on flow fields in the context of NFM techniques using SWE MacTVD, and of catchment roughness on pollutant transport using Solute MacTVD. This was motivated by the wish to learn more about the impact of rewilding as a countermeasure to the global issues of surface runoff flash flooding and nitrate pollution.

In order to achieve this, the following aims were set:

- Investigate the effect of different roughness values for strip rewilding on runoff flowrate for a uniform slope
- Investigate the effect of macro-roughness on runoff flowrate
- Investigate the effect of catchment roughness on pollutant transport
- Validate and note the limitations of the computational model used, as compared to previous experimental and numerical data

A literature review was carried out to better understand the state of research in the field of NFM modelling. Through this it was determined that an increased roughness approach could work well. It was also found that there was room to research the effect of varying roughnesses on a uniform slope catchment, since previous papers tended to prefer V-shaped catchments and only up to two different roughness values. Not many papers were available about modelling macro-roughness, but there was one paper regarding a steep mountainous catchment that clearly left scope for exploration in lowland settings. Finally, pollutant transport papers were found to be idealised, or over-emphasising infiltration and mixing effects, which is not applicable to surface runoff floods. Therefore, a real catchment was analysed looking only at runoff effects.

The mathematical and numerical basis and setup of SWE MacTVD was briefly discussed, before some key limitations were pointed out: SWE MacTVD cannot model very thin flows and therefore struggles with steep gradient changes. This means it cannot perfectly model an overland plane catchment.

Having pointed out the limitations, SWE MacTVD was then set up to replicate some past 1D uniform slope cases in order to verify its accuracy. Correlation between the model and experimental data was good for a uniform roughness and the varied roughness case was equally consistent. There were minor, but explainable, deviations from experimental data.

After validating the model, SWE MacTVD was used to examine the effect of changing the roughness of a strip across a uniform slope catchment. The results showed that the increased section of roughness caused regions of reduced gradient magnitude on both the rising and falling limbs. Furthermore, with increasing roughness, time of concentration increased, and peak discharge decreased, both with diminishing returns.

The next experiment was an investigation into the effect of macro-roughness on a uniform slope, generated by superposing a cosine wave onto the catchment height values. Increasing magnitude in a periodic macro-roughness slope reduces the maximum runoff and prolongs the time of concentration, but the scope of the analysis was limited by the model's numerical stability. An optimum frequency coefficient of $0.55m^{-1}$ was found for this particular case.

SWE MacTVD and Solute MacTVD were then validated against the velocity and transport modelling data of the Thies catchment respectively. SWE MacTVD generated plots very similar to simulations run by Mügler et al. and comparison with experimental data showed a strong correlation to proportionality between SWE MacTVD-modelled and experimental velocities. Application of this velocity data to Solute MacTVD generated a convincing evolution of concentration contours for both injection points D and E. Comparison of Solute MacTVD solutions with experimental and simulated data showed good correlation.

The catchment roughness was then altered to investigate the impact of roughness on pollutant transport. The overall trend observed across both points was that the higher the roughness of the catchment, the longer it took for pollutant to travel to the outlet. Furthermore, aside from the result for point E at roughness 0.03, it appeared as though there was also a trend that the higher the roughness, the lower the peak concentration. These catchment roughness results were then compared with simulation data from Mügler et al. All data was in agreement aside from the result for point E at roughness 0.03, whose validity could be called into question, considering that the simulated data conforms with the hypothesised trend.

Contents

Technical Abstract i

Contents iii

1 Introduction 1

1.1 Overview 1

1.2 Motivation 1

1.3 Aims 2

2 Literature Review 3

2.1 Modelling Surface Roughness 3

2.2 Modelling Rewilding 4

2.3 Macro-roughness 6

2.4 Pollutant Transport 7

3 Flow Field Simulation 9

3.1 Overview 9

3.2 Mathematical and computational model 9

3.3 Model Setup 10

3.4 Limitations 11

3.4.1 Outlet Boundary Condition 11

3.4.2 Depth Instability 12

3.5 Validation 13

3.5.1 Validation for 1D Uniform Roughness 13

3.5.2 Validation for Varied Roughness 14

3.6 1D Roughness Strip Experiment 15

3.7 Macro-Roughness Experiment 18

3.7.1 Varying Magnitude 19

3.7.2 Varying Frequency 20

4 Solute Transport Simulation 23

4.1 Overview 23
4.2 Mathematical and computational model 23
4.3 Base Case Catchment and Experiments 24
4.4 Model Setup 25
4.5 Validation 26
4.5.1 Validation of Flow Field 26
4.5.2 Validation of Solute Transport...30
4.6 Catchment Roughness Effects 34
4.6.1 Point D 34
4.6.2 Point E 36
4.6.3 Summary 36
4.7 Comparison to Mügler et al 36
5 Conclusions 38
6 References 40
A) Symbol Definitions 45
B) Risk Assessment Retrospective 46

1 Introduction

1.1 Overview

In this report, the effect of variation of surface roughness on the runoff flow field and pollutant transport has been investigated by use of two computational models (SWE MacTVD and Solute MacTVD). SWE MacTVD has been validated against a number of experimental and numerical cases, before being applied to draw conclusions about how variation in roughness and macro-roughness () affect surface flow in a flood scenario. Solute MacTVD has been validated against a real-world catchment and was then applied to draw conclusions about how catchment roughness affects pollutant transport. These results could then be used to better inform judgements on the implementation of Natural Flood Management (NFM) techniques as a means to tackle the growing issues of flooding and nitrate pollution.

1.2 Motivation

Higher intensity flooding events are increasingly common in the UK. Climate change means that more extreme weather is expected in the future. The IPCC suggests heavier rainfall events in UK are 'very likely', with a 10% increase in rainfall by 2100 (Pidcock, 2014). This, combined with recent relatively high-profile flooding cases across the UK in 2019 (BBC News, 2019; Davies, 2019; Busby, 2019; Sky News, 2019), makes the risk of flooding a significant concern.

Heavy intense rainfall overloads natural and artificial drainage systems leading to 'flash floods'. These are driven predominately by surface runoff over catchments. One potential solution is to increase roughness or unevenness of a catchment to reduce the intensity of surface runoff. This project aims to explore how roughness and macro-roughness variations can affect rainfall runoff and pollutant transport in order to bring further understanding for storm event applications.

Rewilding, a form of NFM, is the process of returning a catchment to natural conditions, often leading to an increase in vegetation density and thus an increase in the effective roughness of a catchment. Such an example can be found in a case in Wales, where replacing pastures with forest reduced surface runoff by up to 78% (Carver, 2016). It is also well documented that plant-based measures are effective at controlling soil erosion and providing stability to the sediment (Yan, et al., 2018).

Another implementation of NFM comes in the form of in-ditch barriers, sediment traps (SEPA, 2015) and swales (Susdrain, 2020). These forms of NFM act as macro-roughness generators by altering the topography of a catchment above the sedimentary scale. Although these techniques are primarily used for water or sediment retention, they also have a secondary impact on runoff nonetheless, especially if multiple rows are employed. The effectiveness of swales can be augmented through the use of dams or filter strips (Davis, Stagge, Jamil, & Kim, 2012).

Nitrate contamination is widely regarded as one of the major problems for the aquatic environmental around the world (Nestler, et al., 2011; Collins, Stutter, & Kronvang, 2014), due to the possibility of leading to issues such as eutrophication. In a recent study, agricultural runoff from Hunan, Hubei and Sichuan accounted for 10.1%, 9.8% and 9.2% to the total local freshwater eutrophication potential (Huang, Xu, Ridoutt, Wang, & Ren, 2017). With increased storm event frequency, nitrates and other ions are at increased risk of being transported and building up downstream, which can have a negative outcome on local wildlife. Experimental results show that just by using strips of cover crop, runoff losses via pollutant transport can be cut by up to 80% as compared to bare compacted soil (Burguet, Guzmán, de Luna, Taguas, & Gómez, 2018).

1.3 Aims

In order to help tackle these issues and further expand on the understanding of utilising roughness measures on surface runoff properties, the following main points of interest are identified as aims for this project:

- Investigate the effect of different roughness values for strip rewilding on runoff flowrate for a uniform slope
- Investigate the effect of macro-roughness on runoff flowrate
- Investigate the effect of catchment roughness on pollutant transport
- Validate and note the limitations of the computational model used, as compared to previous experimental and numerical data

2 Literature Review

2.1 Modelling Surface Roughness

As well as manually inputting roughness values into a computational model, it is common to model obstructions purely by using net exclusion and topography (Cea, Garrido, & Puertas, 2008). Cea et al. used these principles in validating their hydraulic model, relying on the removal of mesh elements to model obstructions. An example of this can be seen in Figure 1, where walls in a catchment have been modelled by removing the relevant sections of the computational mesh.

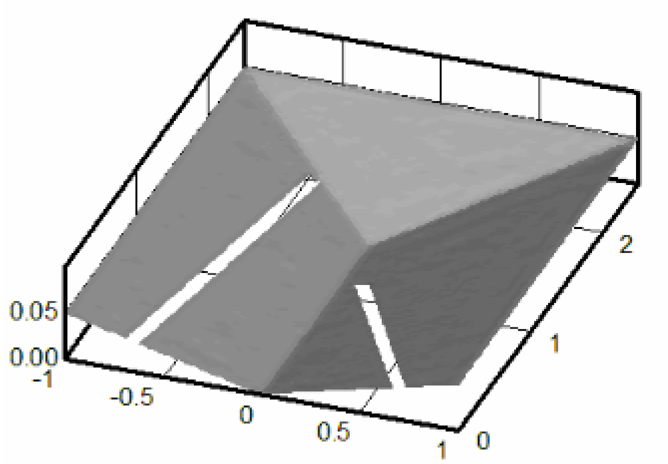

Figure 1 - 3D plot of a catchment with intersecting walls produced by net exclusion (Cea, Garrido, & Puertas, 2008)

Cea et al. formalised these concepts in a later report (Cea, Garrido, & Puertas, 2010), where the concepts of the Building Hole model(BH), shown in Figure 2a, and the Building Block model(BB), shown in Figure 2b, were introduced. In the BH model, obstructions to the flow are modelled by holes with slip walls at the boundaries, whereas the BB model uses detailed 3D reconstructions of every building using LIDAR. The BH model turned out to be more efficient with a less precise mesh, but the trade-off is that a number of real-world nuances are lost, such as for example water draining off the rooves of the buildings back into the catchment.

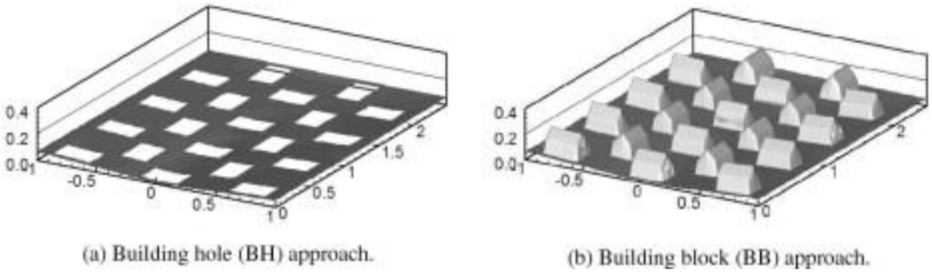

Figure 2 - 3D plots of buildings represented by the BH and BB models (Cea, Garrido, & Puertas, 2010)

In their Masters' project (Chan, 2012), Chan also observed the work of Cea et al. (Cea, Garrido, & Puertas, 2010) and came to a similar conclusion to Cea that a BH model should be used for modelling disruptions to the flow at an urban drainage level of analysis given its computational cheapness. However, Chan also introduces the idea of an increased roughness model, where buildings are replaced by footprints of greatly increased surface roughness, so that perhaps roughness can act as an alternative method for modelling irregularities in a surface.

This increased roughness was not explored in depth by these papers and will be explored in this project: the BH model, while efficient, is not totally true to the real scenario; an accurate implementation of the BB is computationally expensive.

2.2 Modelling Rewilding

A paper which heavily inspired this project is Wallace's Masters' project (Wallace, 2019), in which the effects of rewilding were modelled and explored. Utilising the same computational model that will be used for the first section of this report, it focussed on the implementation of horizontal rewilding bands to the V-shaped catchment shown in Figure 3, and specifically how rewilding area, location, and fragmentation affected rainfall runoff.

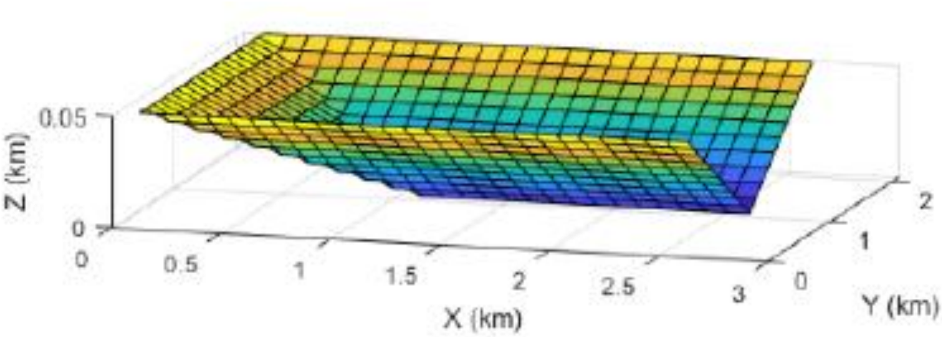

Figure 3 - V-shaped catchment as used by Wallace (Wallace, 2019)

The main conclusions arrived from Wallace were:

- Increasing the rewilded area linearly increased the time of concentration (the time taken for a rainfall event to produce maximum discharge) assuming the band remained in the same position. Adjusting area while shifting the average position had non-linear effects.
- The shorter the distance between rewilding bands and the outlet, the larger the time delay imparted on the time of concentration. Adversely, this also causes a larger local water depth which maybe cause flooding.
- Fragmentation has no discernible effect on rainfall runoff characteristics.

Extensions to Wallace's project that will be explored in this project include the changing of the catchment shape from a V-shape to a uniform slope, as well as an investigation into the impact of varying rewilding strip roughness on rainfall runoff properties.

Hou et al. is in close agreement with Wallace's conclusions. (Hou, et al., 2018) A study was performed on a V-shaped catchment using two types of surface: forested and grassland. It was found that, as found by Wallace, roughness fragmentation had no real impact on surface runoff. It was also found that placing forest surface closer to the outlet increased the time of concentration, but also the local water level, again much in agreement with Wallace. In fact, this conclusion is also drawn by Wong and Li (Wong & Li, 1998), whose study into urbanisation scheduling determined that leaving the rough non-urbanised land nearer the base of the catchment until last was optimal for delaying flooding events. A limitation of these studies is that they do not distinguish themselves from Wallace's project in terms of catchment shape and roughness effects: they are still V-shaped catchments with a maximum of two roughness values.

Some papers that explore different catchment shapes include that by Wu et al. (Wu, Woolhiser, & Yevjevich, 1982), which looked into the effect of roughness layouts on runoff for a concave section, and that by Maske & Jain (Maske & Jain, 2014), which looked at another two different catchment shapes with varied roughness values but an identical average, as detailed in Figure 4. Both draw conclusions about how roughness distributions affect peak discharge and time of concentration. However, what is missing from both is an investigation into how changing the roughness values themselves will affect the runoff: Wu et al. constructed all catchments out of only two different materials, whilst Maske & Jain varied roughness values both linearly and randomly, yet never changed the average value.

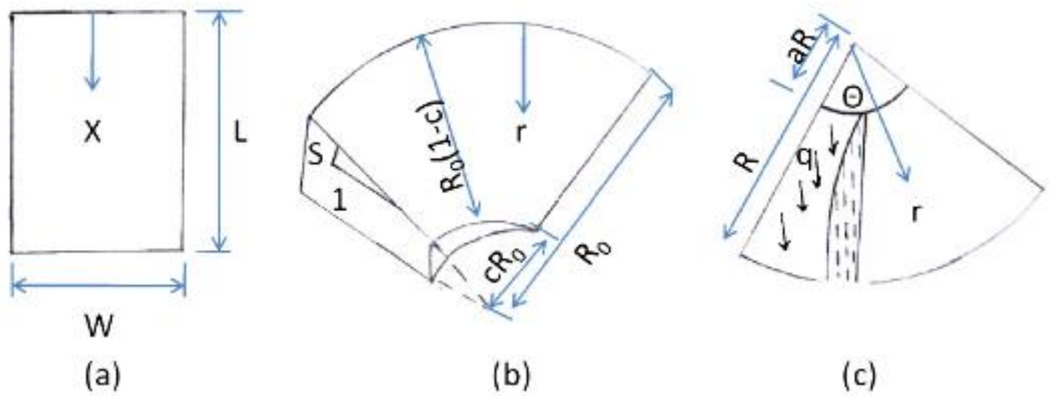

Figure 4 - Three types of catchment shapes covered by Maske & Jain and Wu et al.: (a) rectangular plane (b) converging section (c) diverging section (Maske & Jain, 2014)

Finally, another roughness experiment worth mentioning is that performed by Ferreira et al. in which a soil rectangular plane had different spatial arrangements of impermeable pavement slabs and was tested under rainfall events (Ferreira, et al., 2019). In a way, urbanisation is analogous to a form of reverse rewilding, in which pavement takes away vegetation. Again, however, this paper did not examine varying roughness levels, sticking with only two distinct roughness values, namely the soil and the pavement. This still leaves room when investigating a rectangular catchment to understand the effect of varying the roughness level of the rewilding surface.

2.3 Macro-roughness

Studies into the hydrological effects of introducing macro-roughness measures are sparse, with the majority tending to be analyses of trenches for use in highway applications (Davis, Stagge, Jamil, & Kim, 2012; Leroy, et al., 2016; Rujner, Leonhardt, Marsalek, & Viklander, 2018). These applications tend to focus on transit-caused pollutants and sedimentation effects and are therefore not very applicable to flash flooding and

One recent study into macro-roughness effects looked at how dip slopes affected runoff in a mountainous catchment (Gan, He, & Qin, 2020). Gan et al. used experimental data from sites whose catchments slopes were angled between 11° and 31°, comparing dip and anti-dip slopes at varying angles. It was concluded that rock dip angles in both orientations, as well as rainfall intensity, had the largest impact on the measure surface flow velocity. These conclusions apply well for mountainous regions such as that shown in Figure 5 with high slope gradients, as well as exposed and angled stratified rock layers to provide the macro-roughness.

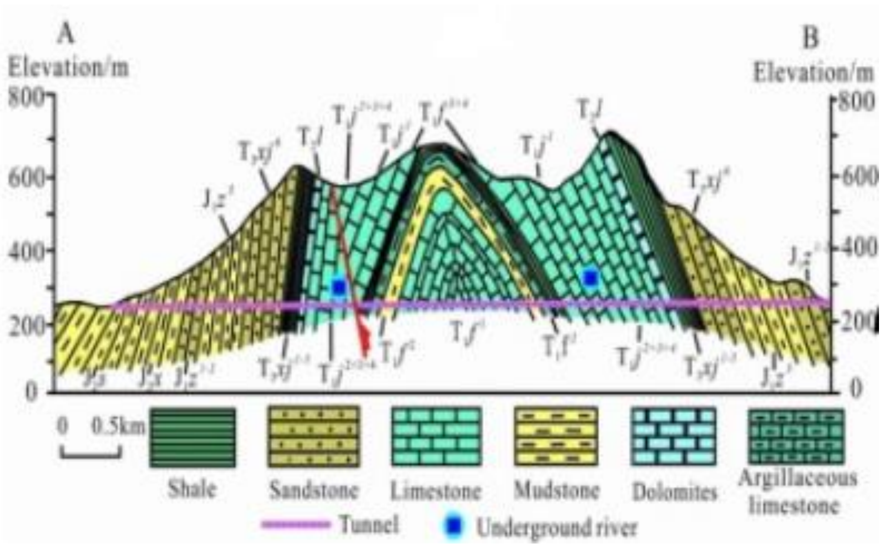

Figure 5 - Stratified rock geology of site in China studied by Gan et al.

Nevertheless, this still leaves the effect of macro-roughness in less drastic lowland catchment topographies, such as periodic trenching in a catchment, unexplored. This project will investigate how macro-roughness impacts runoff for a catchment in a non-mountainous less steep region.

2.4 Pollutant Transport

It is worth noting that Ferreira et al., whom were previously discussed regarding the experimentation with impermeable plate arrangements, also included sediment transport study in the same paper (Ferreira, et al., 2019). However, these results were less than conclusive, being limited by the laboratory scenario: the only ‘pollutant’ was the sediment itself and the sediment layer was only 5cm thick, meaning once it had eroded away the results ceased to be reliably applicable to a real-world catchment.

The predominant method for modelling the transfer of soluble pollutants to surface runoff is the mixing layer model popularised by Lehman & Ahuja (Lehman & Ahuja, 1985). The idea is that when a raindrop impacts soil, a certain depth of the soil gets kicked up and is mixed with the raindrop via accelerated diffusion. This concept has been extensively numerically validated (Dong, Wang, Zhou, & Shan, 2013; Gao, et al., 2005). The issue with this model for the application to flash flooding is that in such an extreme rainfall case the soil quickly becomes effectively saturated and there is little time or room for mixing to occur. Therefore, in this project, only surface flow effects on pollutant transport will be considered.

In terms of papers that considered the effects of sustained rainfall, the majority seemed to be agricultural in nature. For example, Walton et al. (Walton, Volker, Bristow, & Smettem, 2000) studied the effect of sustained rainfall on pre-planted bromide tracer in an agricultural setting, studying soil columns as well as plane catchments. However, these tests did not pre-wet the catchments to saturation, and therefore pollutant transport was heavily influenced by infiltration, seepage, and surface pooling. It was found that solutes in this scenario had a strong tendency to be absorbed downwards into the soil. A number of papers have corroborated this tendency for solutes to have a large preference for vertical rather than lateral flow (Lamb, et al., 2019; Havis, Smith, & Adrian, 1992). Nevertheless, as mentioned before, in this report a saturated condition is assumed and therefore negligible infiltration occurs to allow vertical flow.

Finally, a good example of an impermeable flow experiment is that by Xiao et al. which experimentally investigated the concentration of salt solution over time at the outlet of a catchment during a rainfall event (Xiao, Zhang, Liang, & Chen, 2016). This yielded some clear results regarding surface flow pollutant transport:

- Lower surface roughness reduces time of concentration.
- Higher rainfall intensity reduces time of concentration.

However, this experiment is highly idealised and if possible, such experiments will look at the effects of surface runoff pollutant transport on a realistic catchment, such as the one this report will detail later.

3 Flow Field Simulation

3.1 Overview

The first area of rainfall modelling undertaken was to implement and verify a computational model for surface flow velocities. The results of previous experimental and numerical experiments were used as a comparison to check for validity of the model, from which conclusions about its accuracy were drawn. After validating and accommodating for inaccuracies in the model, it was set up in a way to test the effects of differing horizontal strip roughness on a sloped catchment. It was then set up to investigate macro-roughness by varying the catchment topography. These results were used to draw conclusions about the implementation of rewilding and artificial roughness on a uniform sloped catchment.

3.2 Mathematical and computational model

For this paper, the Shallow Water Equations (SWE) will be utilised to model the surface flow generated by runoff. It is assumed that there is no infiltration, as is effectively the case in saturated soils during storm events or modern concrete-paved built environments.

By depth averaging the vertical velocity, a two-dimensional (2D) approximation of fluid flow can be derived from the Navier-Stokes equations. This is valid since the magnitude of the depth of surface flows is generally much smaller than the dimensions of the catchment area, such that minimal momentum is transferred in the flow vertically. The flow field can then be derived from Conservation of Mass (1) and Conservation of Momentum in the x (2) and y (3) directions, as described by Liang et al. (2006) in the following equations (symbol definitions in Appendix A):

$$\frac{\partial \eta}{\partial t} + \frac{\partial q_x}{\partial x} + \frac{\partial q_y}{\partial y} = 0 \tag{1}$$

$$\frac{\partial q_x}{\partial x} + \frac{\partial\left(\frac{\beta q_x^2}{H}\right)}{\partial x} + \frac{\partial\left(\frac{\beta q_x q_y}{H}\right)}{\partial y} = -gH\frac{\partial \eta}{\partial x} - \frac{g q_x \sqrt{q_x^2 + q_y^2}}{H^2 C^2} \tag{2}$$

$$\frac{\partial q_y}{\partial y} + \frac{\partial\left(\frac{\beta q_x q_y}{H}\right)}{\partial x} + \frac{\partial\left(\frac{\beta q_y^2}{H}\right)}{\partial y} = -gH\frac{\partial \eta}{\partial y} - \frac{g q_y \sqrt{q_x^2 + q_y^2}}{H^2 C^2} \tag{3}$$

In order to computationally solve the fluid flow, a model (SWE MacTVD) based on the Total Variation Diminishing (TVD-) MacCormack scheme proposed by Liang et al. (Liang, Falconer, & Lin, 2006) was applied to the 2D SWE. This scheme makes use of a finite difference method to numerically solve the SWE with 2nd order accuracy in both time and space, advancing the development of the fluid velocities using a certain time step. The TVD adaptation of MacCormack scheme reduces spurious oscillations from the model. More details and basic validation of the TVD-MacCormack scheme can be found in the papers by Liang et al. (Liang, Falconer, & Lin, 2006; Liang, Lin, & Falconer, Simulation of rapidly varying flow using an efficient TVD-MacCormack scheme, 2007).

3.3 Model Setup

In order to calculate a flow field, SWE MacTVD requires a number of inputs about the scenario: the topography of the catchment, roughness values, initial and boundary conditions, and a description of the rainfall event. As well as this, a time step had to be carefully chosen based on the Courant-Friedrich-Lewy (CFL) condition, to maintain the stability of the model.

The catchment topography and roughness were defined using the input text file by assigning a height and roughness value for each cell of the catchment grid. A rainfall event was also described in this text file, detailing the intensity profile over time of a rainfall event over the entire catchment.

In this section, the overland plane model is used due to existing literature using the same model, so that it is a good base model for later comparison. It is characterised by a rectangular sloped plane with a free end at the outlet, as shown in Figure 6.

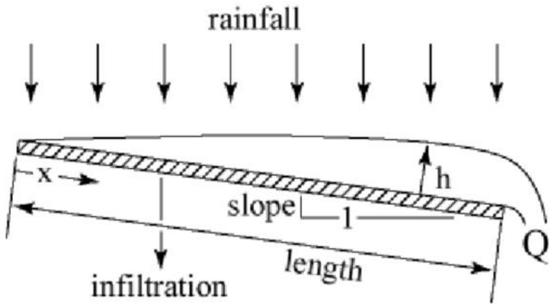

Figure 6 - Diagram showing a crossflow section of an overland plane model (Semmens, et al., 2007)

To determine a stable time step, the CFL condition (4) was used (Wallace, 2019)(symbol definitions in Appendix A):

$$\Delta t \leq \frac{C_0 \Delta x}{v} \tag{4}$$

Where in this case, the Courant number, C_0, takes the value of 1 due to the explicit nature of the computational scheme. The value of the time step constraint can be estimated prior to obtaining results by considering likely values for peak velocity. It is also advantageous to ensure that the time step is not too small, since a smaller time step means more calculations required per given simulation time, leading to a calculation that may be excessively expensive.

3.4 Limitations

3.4.1 Outlet Boundary Condition

The overland flow scenario used in both validation cases requires a free boundary at the outlet, which is essentially a sheer drop at the outlet plane as shown in the catchment in Figure 6. While this sheer drop could not be implemented for stability reasons explained in the next section, an approximation could be made; where the original tests used an overland plane model, the SWE MacTVD case could mimic this with a steepness discontinuity at the outflow as shown in Figure 7. It is important to note this steeper extension to the catchment extends beyond the original such that the outlet lies at the discontinuity.

By not including this extension, SWE MacTVD would default to assuming that the slope effectively continues past the outlet plane. A comparison between runoff curves for a 100m long, 0.01 slope, one dimensional (1D) catchment with constant roughness 0.01 in response to a constant 10mm/hr rainfall event at a cell size of 0.5m with and without the 0.02 slope extension can be found in Figure 8. It can be seen that adding the extension slope does have

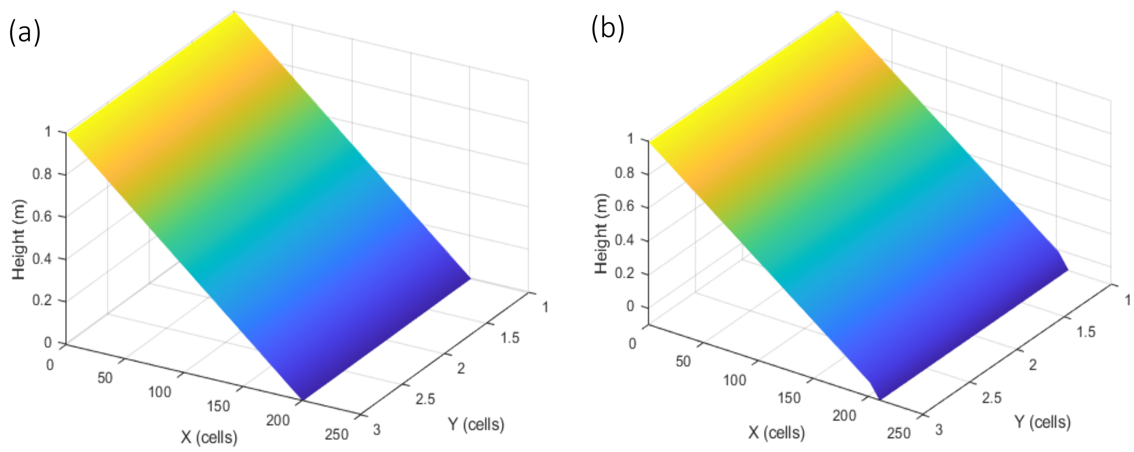

Figure 7 - Comparison of slope topography without (a) and with (b) an extension slope past the outlet

an effect; without the extension (red), the peak discharge is calculated to be lower and the time of concentration is slightly delayed as compared to with the extension (blue). This results from the higher velocity at the outlet as the gradient past the catchment tends towards a sheer drop, leading to rainfall arriving sooner and at a greater magnitude.

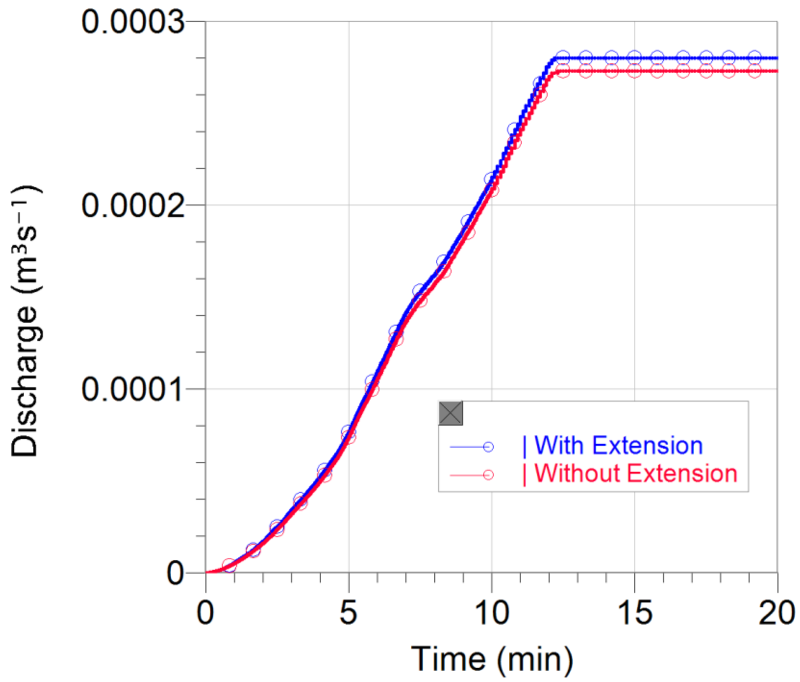

Figure 8 - Hydrograph showing discharge against time with and without extension slope

3.4.2 Depth Instability

When attempting to solve the outlet boundary condition issue, it was observed that there are limitations to the geometry within the catchment, more specifically to the gradient of the slope. The higher the gradient, the faster the fluid flows and therefore the thinner the layer of fluid is. This is an issue since the numerical model uses variable with finite precision and so a water depth too low would be interpreted as having zero depth, causing errors in the calculations.

A demonstration of this can be seen in Figure 9a, where a 105m slope at a cell size of 0.5m has a gradient of 0.01 up to 100m where it changes to 0.05 until the outlet. Figure 9b shows a snapshot of the velocity in the x direction upon application of constant rainfall, produced using Tecplot. It can be clearly seen that the gradient change at 100m leads to instability to arise downstream, as well as up to 3m upstream, indicated by the presence of the chaotic velocity profile; it would be expected that without instability the profile would be a smooth

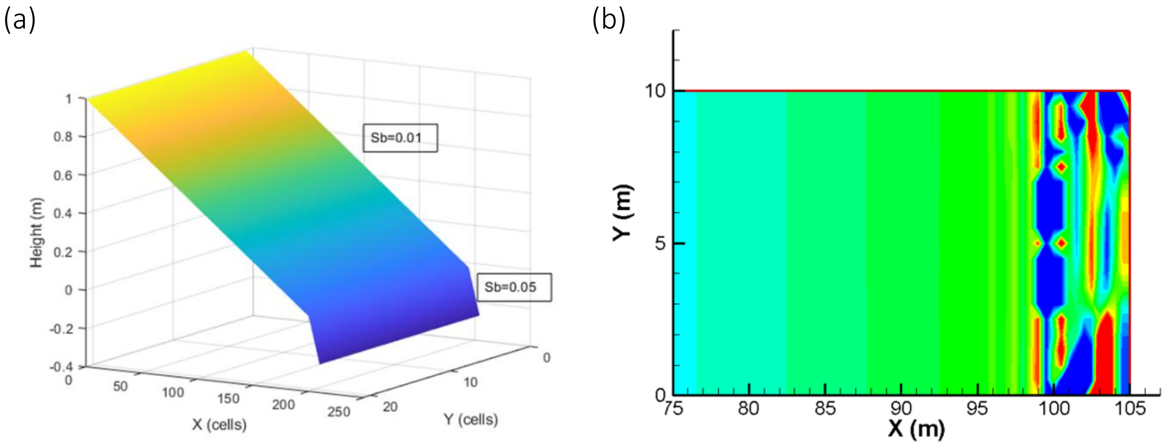

Figure 9 - Sudden and large gradient change (a) topography and (b) velocity snapshot

gradient. This issue was also found in the macro-roughness experiment, where large oscillations relative to the wavelengths created localised areas of high gradient in each trough of the slope function.

3.5 Validation

3.5.1 Validation for 1D Uniform Roughness

One-dimensional uniform roughness slope experiments are well-documented, and thus act as a good base case by which to initially test the validity of SWE MacTVD. One such previous experimental case consists of a one-dimensional uniform slope of length 21.945m, slope

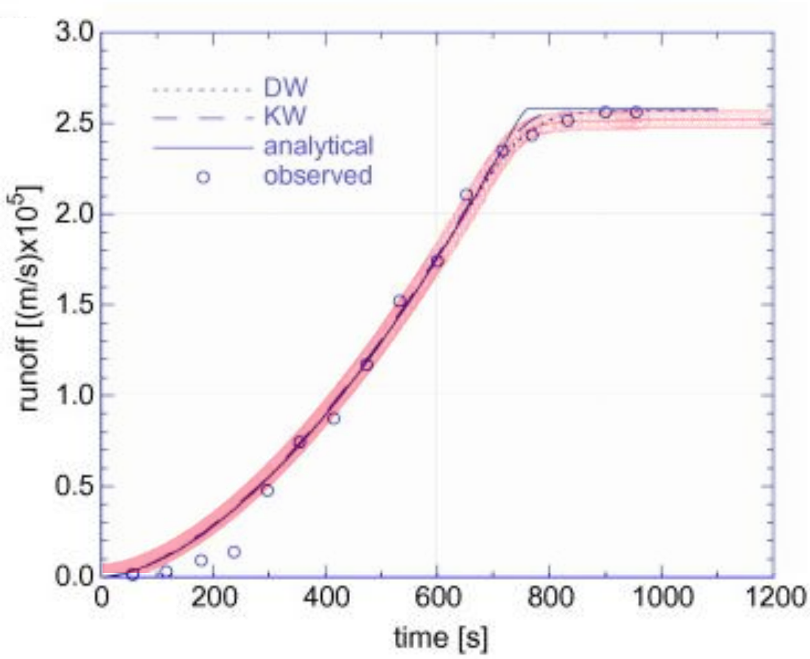

Figure 10 - Uniform slope constant rainfall hydrograph results from SWE MacTVD as compared to previous data

0.04, Manning roughness 0.05, and with a rainfall event of intensity 2.58233×10^{-5} m/s until steady state (Gottardi & Venutelli, 2008).

The results of the simulation are shown as a hydrograph in Figure 10, with SWE MacTVD in red and previous experimental and numerical results in blue. Comparing SWE MacTVD to the numerical data (dotted and dashed blue lines), there is strong correlation throughout the rising limb, with steady state runoff settling at a slightly lower level.

Comparing SWE MacTVD to the observed experimental results, aside from the very start of the rising limb, there is also a strong correlation. The deviation at the start could, as also suggested by Gottardi & Venutelli, be explained by real-life effects such as interception by grass surfaces and a catchment that is not fully impermeable. Nevertheless, the good correlation with experimental results and the numerical hydrographs generated by Gottardi & Venutelli indicates that SWE MacTVD in this case is a valid model.

3.5.2 Validation for Varied Roughness

Since the testing of a roughness strip requires the model to handle flows over a catchment with varied roughness, the next validation step was a comparison to varied roughness cases, where roughness was varied between a range of Manning's roughness values. A unit width slope of length 100m, slope 0.01, and rainfall intensity of 10mm/hr was used for a rainfall

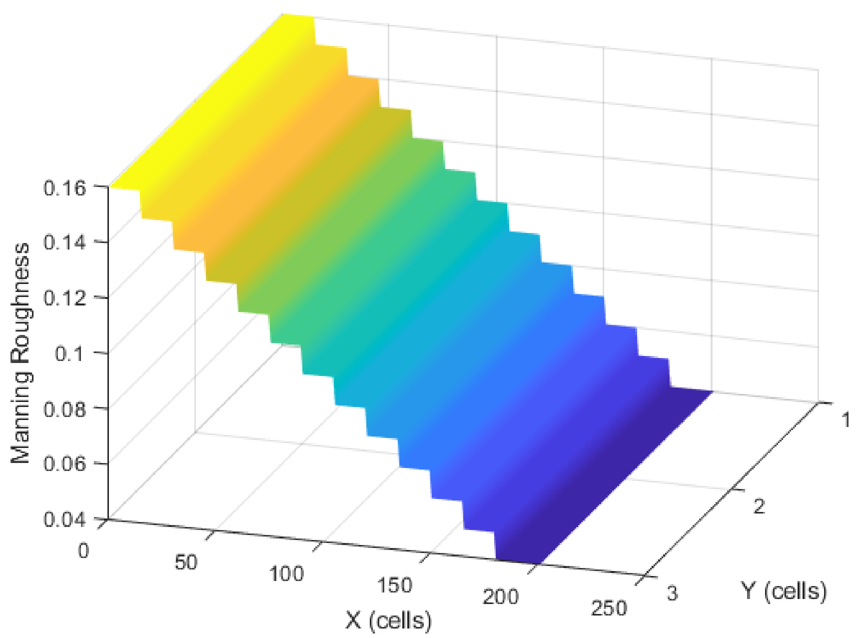

Figure 11 - Manning roughness distribution over catchment for varied roughness validation

duration of 100min and 30min (Huang & Lee, 2009). In both cases, a descending Manning's roughness range of 0.04 to 0.16 and a cell size of 0.5m was used to model the flows, as shown in Figure 11.

The results of these simulations are shown in Figure 12, with SWE MacTVD in red. For the 100 min case in Figure 2a, where rainfall lasts longer than the time of concentration, there is a strong correlation to existing data. In the 30 min case, Figure 2b, while the rising limb correlates well, there is a slight increase in discharge just after rainfall stops and a corresponding slight decrease in the tailing end of the falling limb. This seems to indicate that perhaps the catchment is modelled as slightly less rough than in Huang and Lee's results. The cause may be due to how the outflow boundary condition is defined, as is further explained in the limitations section.

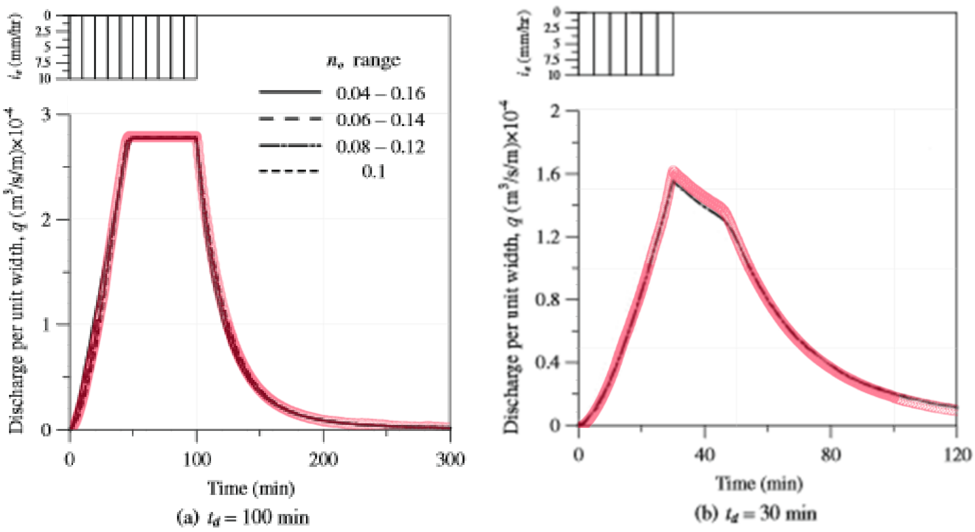

Figure 12 - Varied roughness hydrograph results from SWE MacTVD as compared to previous data for a rainfall event of (a) 100min (b) 30min

3.6 1D Roughness Strip Experiment

After validating that SWE MacTVD is valid for uniform slopes of varied roughness, it is viable to experiment with roughness strips in order to build on the work by Wallace done on modelling rewilding patterns (Wallace, 2019). In this case, the effect of changing the Manning roughness of a strip in the centre of a uniform slope catchment on the time-progression of discharge at the outlet will be investigated.

The results of this 1D experiment are assumed to hold true for a 2D uniform slope catchment since, in the crossflow direction, such a catchment is homogenous and therefore will not interact with itself.

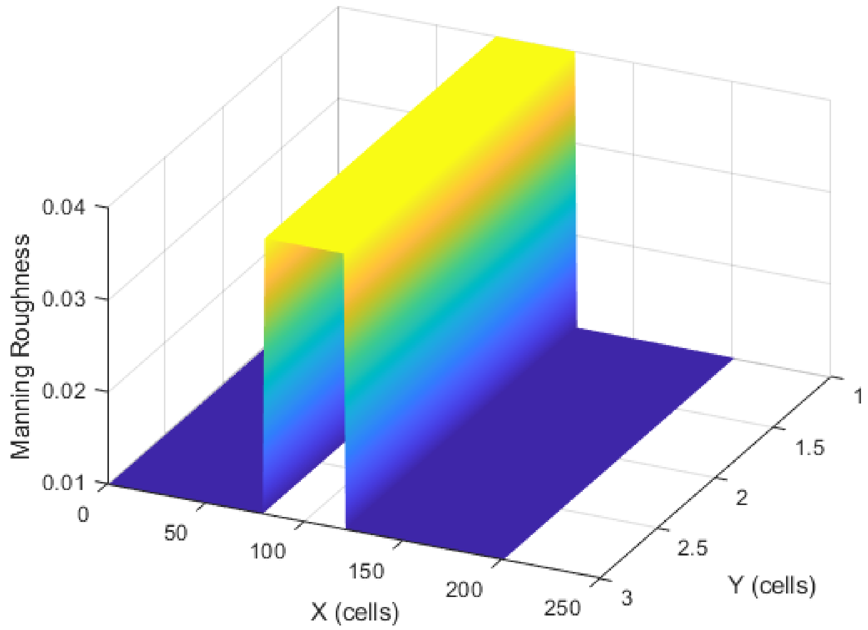

Figure 13 - Example Manning roughness distribution over catchment for roughness strip experiment

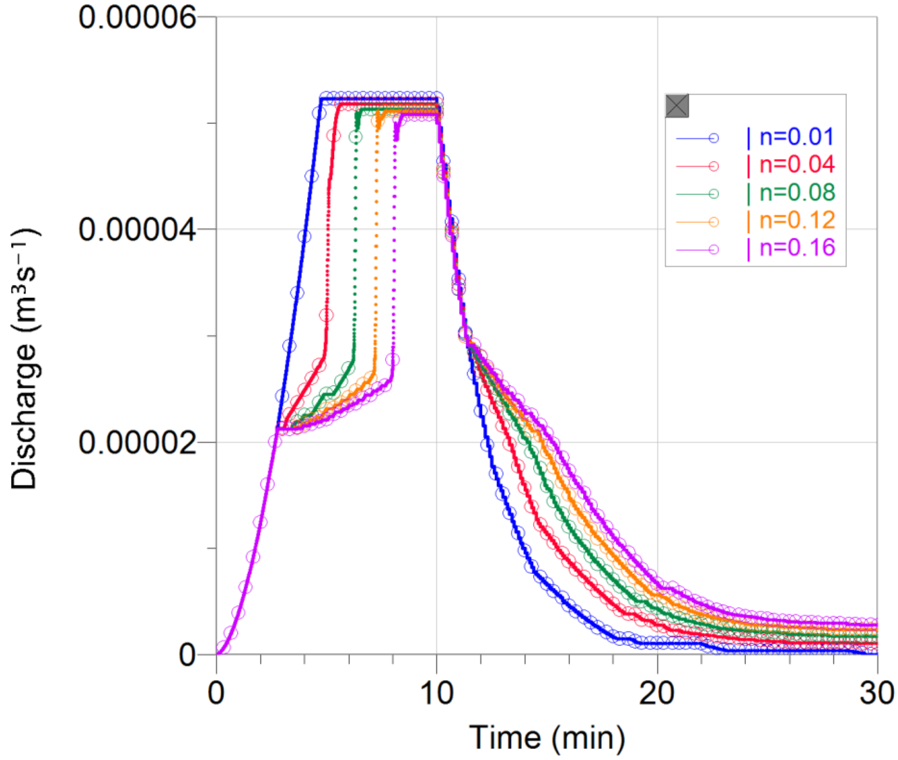

Figure 14 - Roughness strip experiment hydrograph results from SWE MacTVD for a range of different strip roughnesses

This experiment used a 20m long, 0.01 slope uniform catchment of unit width at a 0.1m cell size. Applied to it was a 10mm/hr rainfall event for 10 minutes. The roughness of the catchment was uniform at a Manning roughness of 0.01 aside from a 4m wide roughness strip lying perpendicularly across the flow direction halfway downstream. This roughness strip was tested for a range of Manning roughness values between 0.01 and 0.16. An example roughness profile for the catchment is seen in Figure 13, in this case for the catchment where the roughness strip has Manning roughness 0.04.

The discharge over time at the outlet of the catchment for each of the roughnesses tested is presented in Figure 14. Note that a strip roughness value of 0.01 corresponds to a catchment with no roughness strip.

The main difference between the curves starts at discharge levels just above 2 $x10^{-5}$ m^3s^{-1} on the rising limb and just below 3 $x10^{-5}$ m^3s^{-1} on the falling limb. In these regions the magnitude of the rate of change of discharge reduces the higher the roughness of the roughness strip is. This is because the roughness strip can be seen as a form of temporary storage: rainfall is 'held back' by the region of increased roughness. Therefore, the fast response of the curves prior to this discharge level can be explained by the volume of water that falls downstream of the roughness strip and is unaffected by it. After being slowed down by the roughness strip, the curves then resume at rates equivalent to the 0.01 Manning roughness no-strip case: after these slowed regions, the rainfall upstream of the strip has managed to traverse it.

What is important to note from a runoff perspective is that Figure 14 shows that with an increased roughness, a roughness strip both delays and reduces the magnitude of peak discharge.

The variation of peak discharge and time of concentration against strip roughness are shown in Figure 15. Examining the effect on peak discharge, the magnitude-reducing trend caused by increased roughness is evident. However, the rate at which discharge is reduced falls as the roughness is increased, meaning that at higher roughnesses the returns are reduced. Examining the effect on time of concentration, a similar trend is found, with increased roughness increasing the time of concentration, but also reducing the extent to which it increases. There is again a diminishing return to increasing roughness, albeit to a lesser extent than roughness' impact on peak discharge.

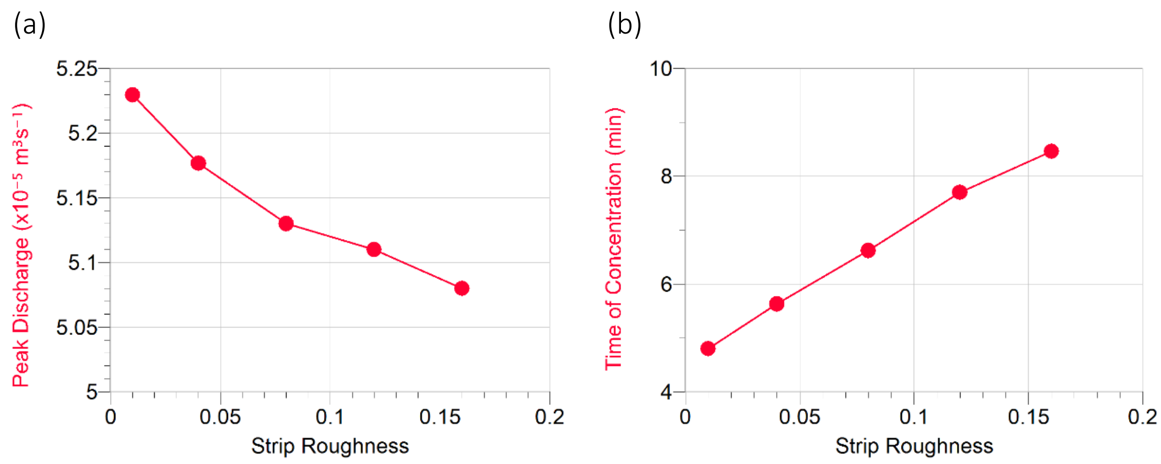

Figure 15 - Plots of (a) peak discharge and (b) time of concentration against strip roughness

3.7 Macro-Roughness Experiment

The effect of macro-roughness was investigated using a variation made to the slope topography of a uniform slope in order to manually produce an uneven surface. In order to do this, a cosine function (5):

$$A\cos(Bx) \tag{5}$$

was superposed with the height values of a uniform slope to generate an oscillating downward-sloping surface, an example of which is shown in Figure 16. The parameters of the slope function that could be altered were the magnitude (A) and frequency (B) of the

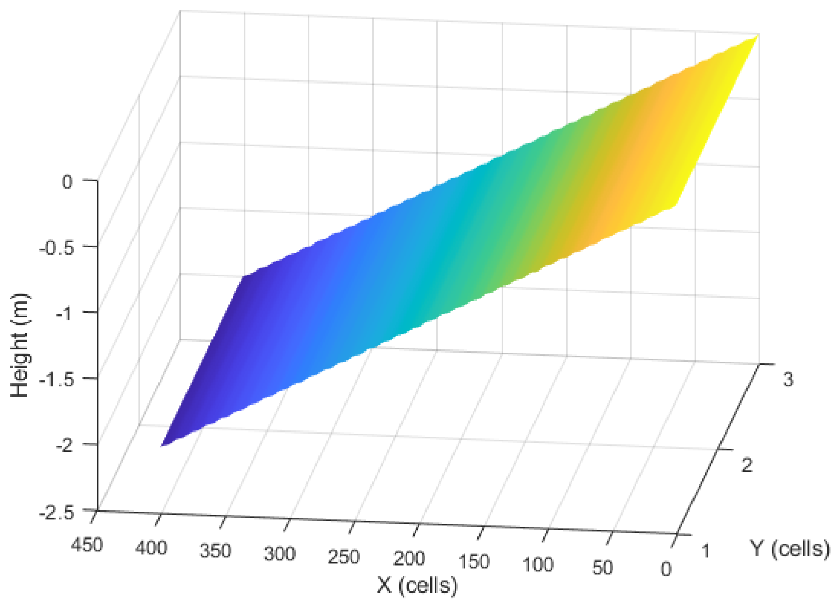

Figure 16 - Representative oscillating slope catchment

oscillation. In all subsequent tests, a unit width slope of length 200m, slope 0.01, cell size 0.5m, Manning's roughness 0.15, and one-hour rainfall event of intensity 10mm/hr was used.

3.7.1 Varying Magnitude

In these test cases, the magnitude coefficient (A) of the additional cosine function was varied from 0m, which is effectively a uniform slope, to a maximum of 0.01m. A frequency coefficient of 0.5m^{-1} was used for all these cases. Magnitudes that are too high cause large oscillations in the surface, creating regions of very small or even positive gradients as seen in Figure 17. This would make the flow in the regions very thin, such that the numerical model would struggle to stably model the flow, as will be elucidated in the limitations section.

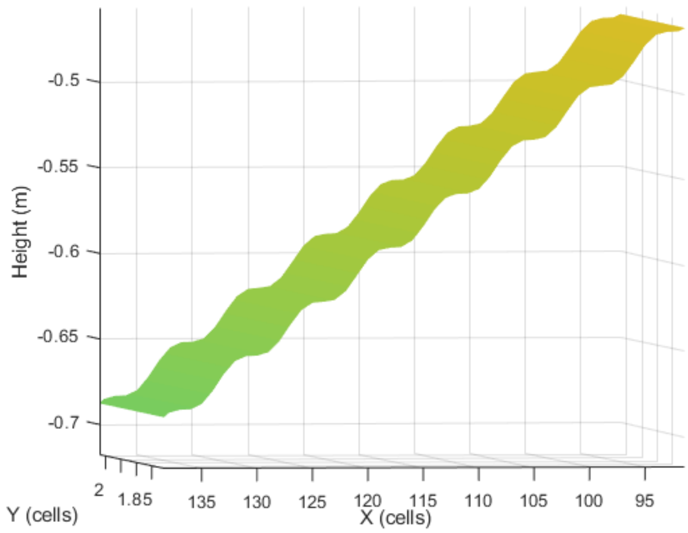

Figure 17 - Slope segment for the case where magnitude was too great relative to a given frequency

The results for a range of magnitude coefficients are shown in Figure 18, with each curve colour representing a corresponding magnitude coefficient as detailed in the legend. The most notable result from this is that, as the magnitude of oscillations increases, the runoff intensity at the plateau decreases and the time to concentration is prolonged. This is offset at the receding limb, where the higher magnitude slopes take longer for the runoff to decay: the runoff curve is flattened, and outflow rates are spread out to a later time. The oscillations on the rising limb of the 0.01m magnitude case should be noted, indicating the onset of instability due to thin flows and thus the fact that the maximum stable magnitude coefficient value was being approached.

This result can be approximately thought of as analogous to the effect of increasing roughness: increasing the magnitude coefficient increases the effective roughness. This increased effective roughness is likely compounded by a combination of two other factors. One factor is that larger oscillations mean that rainfall can be 'trapped' in regions of lower

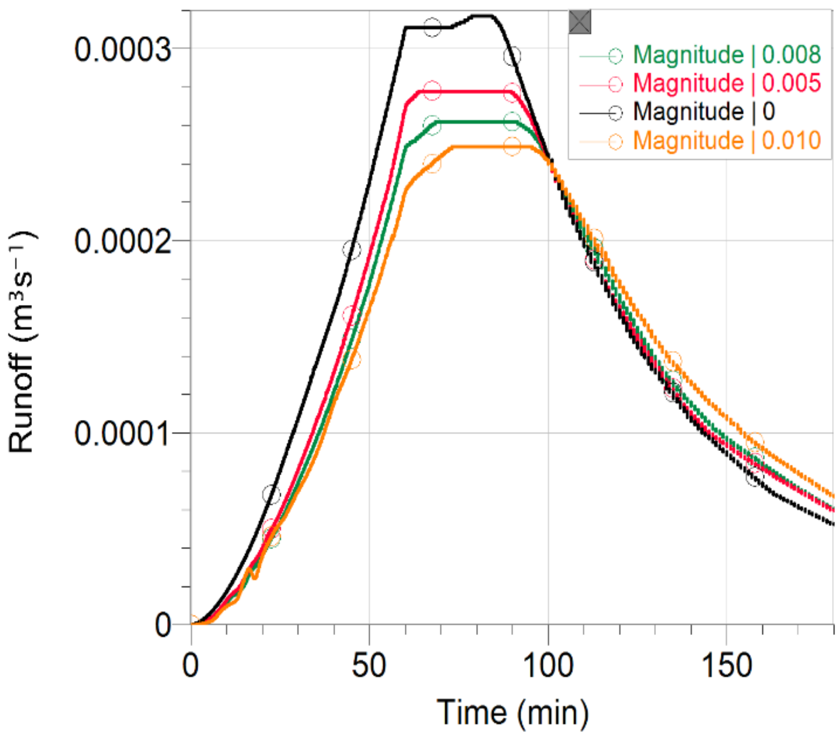

Figure 18 - Resultant hydrograph for varying oscillation magnitude for the macro-rough catchment

gradient, creating regions of surface storage that prolong the time it takes for rain to reach the outlet. The other factor is that the effective slope length is increased with larger magnitudes, meaning there is more distance for rain to flow down.

3.7.2 Varying Frequency

In these test cases, the frequency coefficient (B) of the additional cosine function was varied from 0.1m^{-1} to 1m^{-1}. A maximum limit to the frequency arises due to the resolution of the model being determined by the step size, as shown in Figure 19, where increasing the frequency above this results in the catchment topography not being fully captured. Another limit was that of relative magnitude: as the frequency increases, the maximum allowable magnitude decreases due to the slope gradient limitations discussed above. A magnitude coefficient of 0.001m was used to allow for the stable modelling of all the used frequencies.

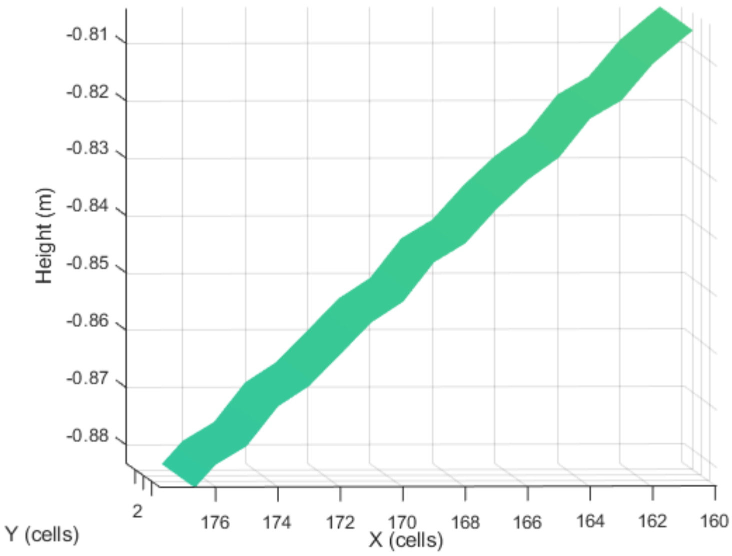

Figure 19 - Slope segment for the case where high frequency caused oscillations with too short a wavelength for the given step size

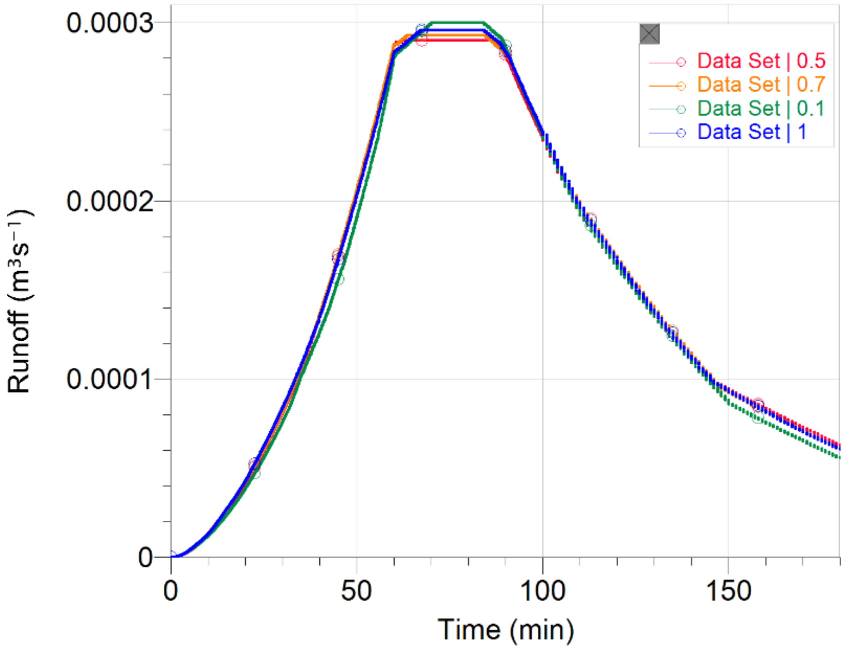

Figure 20 - Resultant hydrograph for varying oscillation frequency for the macro-rough catchment

The results for a selection of these frequencies are shown in Figure 6, with the curve colours corresponding to a frequency coefficient as detailed in the legend. Both a frequency of $0.1m^{-1}$ and $1m^{-1}$ result in greater runoffs than a frequency of $0.5m^{-1}$. A frequency of $0.7m^{-1}$ is intermediate to the $0.5m^{-1}$ and $1m^{-1}$ curves, as would be expected.

A potential explanation for lower frequencies causing high runoff could be that they result in very minimal oscillation, tending towards a flat slope which does not benefit from effective roughness effects. On the other hand, a higher frequency may lead to greater runoff due to increased gradients overcoming the water 'trapping' effect.

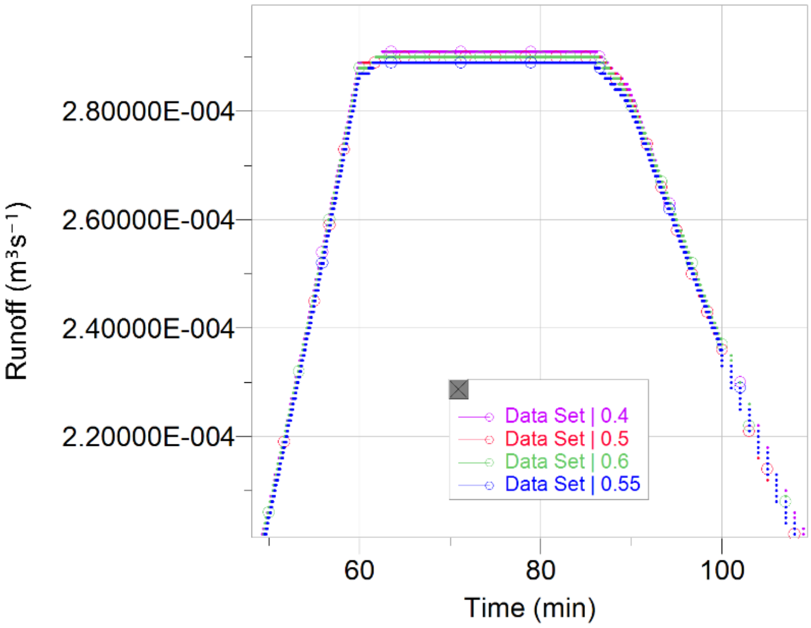

Figure 21 - Detail of plateau of resultant hydrograph for varying oscillation frequency near minimum runoff for the macro-rough catchment

Figure 7 shows a close-up view of the runoff plateau for frequency coefficients around the 0.5m^{-1} range, again with curve colours corresponding to the respective frequency coefficients in the legend. The curves for coefficients of 0.5m^{-1} and 0.6m^{-1} are practically overlapping one another, while the 0.55m^{-1} curve is clearly lower than both. This suggests that, for this test case, an optimum value of around 0.55m^{-1} for the frequency coefficient leads to the lowest runoff. A useful extension to this would be to investigate the effect of frequency on different catchment geometries or rainfall durations to see if these affect the optimal frequency of oscillations for minimising surface runoff.

4 Solute Transport Simulation

4.1 Overview

The second area of rainfall modelling undertaken was to implement and verify a computational model for pollutant transport. This section is heavily based on the experimental and numerical results outlined by Mügler et al. (Mügler, et al., 2011) relating to a real-world surface flow and tracer transport experiment. First, SWE MacTVD and Solute MacTVD were used to model the scenario and compared with the raw experimental data to validate them for this application. This needed to be carried out both for the flow field in the catchment and for the pollutant concentration results at the outlet from tracer experiment. After validating the model, the roughness of the whole catchment was varied in order to determine its effect on pollutant transport times. These results were then used to draw conclusions about the impact of rewilding density on pollutant transport along a catchment.

4.2 Mathematical and computational model

The models for generating the flow velocity fields are the same as those used in the previous section, making use of the SWE and SWE MacTVD.

In order to model the concentration of solute over time, assuming it follows the flow exactly, conservation of solute mass (6) can be used as described by Liang et al. (Liang, Wang, Falconer, & Bockelmann-Evans, 2010) (symbol definitions in Appendix A):

$$\frac{\partial HS}{\partial t} + \frac{\partial UHS}{\partial x} + \frac{\partial VHS}{\partial y} = \frac{\partial}{\partial x}\left(HD_{xx}\frac{\partial S}{\partial x} + HD_{xy}\frac{\partial S}{\partial y}\right) + \frac{\partial}{\partial y}\left(HD_{yx}\frac{\partial S}{\partial x} + HD_{yy}\frac{\partial S}{\partial y}\right) + q_s \quad (6)$$

Where

$$D_{xx} = \frac{\sqrt{g}H\left(\varepsilon_l U^2 + \varepsilon_t V^2\right)}{C\sqrt{U^2+V^2}} \quad (7)$$

$$D_{xy} = D_{yx} = \frac{\sqrt{g}H(\varepsilon_l - \varepsilon_t)UV}{C\sqrt{U^2+V^2}} \quad (8)$$

$$D_{yy} = \frac{\sqrt{g}H\left(\varepsilon_l V^2 + \varepsilon_t U^2\right)}{C\sqrt{U^2+V^2}} \quad (9)$$

By using the operator-splitting technique to create multiple simpler sub-equations based on each dimension, this equation can be solved numerically using MacTVD. More details and validation of this model in pollutant transport applications can be found in the paper by Liang et al. (Liang, Wang, Falconer, & Bockelmann-Evans, 2010).

4.3 Base Case Catchment and Experiments

The catchment that was prepared and experimented upon in Mügler et al, and that will be used as a base case for this section of the report, is a real-world sandy soil surface in Thies, Senegal (shown in Figure 22). The catchment area is 4m x 10m and consists of a slope of gradient 0.01 that had been prepared by raking in a slight V section. The catchment was set up with a rainfall simulator that could supply the whole surface with an approximately constant 70mm/hr rainfall intensity.

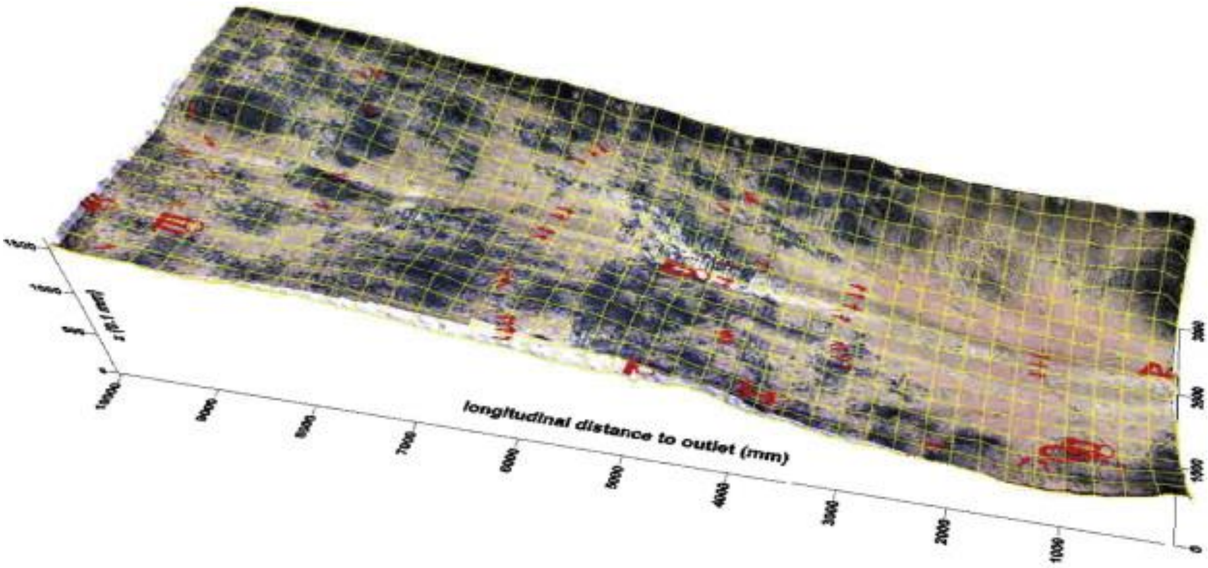

Figure 22 - Topography of Thies catchment (Mügler, et al., 2011)

Mügler et al. conducted two experiments on this catchment: a point-injected tracer experiment ad a surface flow velocity experiment. Results from both of these experiments were used to validate Solute MacTVD as a model for solute transport.

The tracer experiment was conducted first chronologically in order to avoid salts required for the velocity tracking interfering with solute concentration measurements. After prolonged rainfall to wet the catchment and minimise subsequent changes to the topography caused by the rain flow, rainfall was applied to the catchment such that steady state flow was achieved. Then a series of 8 tracer injections were applied to the flow emitting 1g/s over a period of 30s. Periodic samples of the outflow were collected and later tested for conductivity, acting as a proxy for the concentration tracer ions in each sample. (Mügler, et al., 2011)

The surface flow experiment occurred on the conclusion of the tracer experiments. A rainfall event of 135 minutes at an intensity of 70mm/hr was applied to the catchment, such that steady state flow was again achieved. Salt Velocity Gauges were then used to measure the flow velocity in the downstream direction at a number of stations, such that an image of the velocity profile could be constructed. (Tatard, et al., 2008)

4.4 Model Setup

A velocity field for the catchment can be attained through identical means to before, using the SWE MacTVD model. Topography data from the microtopography measurements taken on site was directly input into the model via the input file.

In order for the Solute MacTVD model to operate, two further details are required: a 'HUV' file detailing the water depth and x and y velocities of the steady state flow, and details about the application of the pollutant source. The former can be obtained through some manipulation of the velocity field results, taking values for these variables at a snapshot during any time zone where steady state flow has been achieved. The latter can be directly implemented into the input file, specifying the coordinates of the pollutant source and the time history of the source contribution per unit area.

Another factor that changes for the Solute MacTVD model is that a different equation was used to determine if the CFL condition was met. Both of the following equations must be satisfied for a stable solution to arise (Liang, Wang, Falconer, & Bockelmann-Evans, 2010) (symbol definitions in Appendix A, and equations (7), (8), (9)):

$$\Delta t \leq \frac{C_0 \Delta x}{\sqrt{U^2+V^2}} \tag{10}$$

$$\Delta t \leq \frac{C_0 (\Delta x)^2}{2\sqrt{D_{xx}D_{yy}-{D_{xy}}^2}} \tag{11}$$

The time step value can again be approximated such that it meets the conditions of (10) and (11) but remains relatively large to ensure computation time is not excessive.

4.5 Validation

4.5.1 Validation of Flow Field

The first validation task when modelling the Thies catchment is to verify that an appropriate velocity field is obtained, and thus that the topography has been mapped correctly. This is important to get right as the solute transport solutions directly follow from the steady state flow velocity solution: an error in the velocity field would lead to an error in the concentration calculations.

In order to compare with the results from Mügler et al, a rainfall event of intensity 51.5mm/h was applied to the catchment until steady state was achieved: given the assumption of steady state conditions, it can be assumed that the rate of infiltration is constant and can be subtracted to calibrate the real-world rainfall intensity of 70mm/hr. (Mügler, *email correspondence*, 2012) For this comparison, a constant Manning roughness of 0.02 was applied across the whole catchment.

Figures 23a and 23b show the water depth and velocity fields respectively, as calculated by SWE MacTVD. Figures 23c and 23d show the water depth and velocity fields as found in the paper by Mügler et al.

Comparison of the water depth plots (Figures 23a and 23c) seems to show overall an agreement in the depth profiles, with the topography of the catchment being evidently reflected in both sets of results. There are some visual differences: the high depth area 9.6m down the catchment seems to be larger in the SWE MacTVD results and the width of medium depth flow in the main channel seems less well defined. However, this may all be attributable to the apparent lower resolution of the SWE MacTVD plot which causes some values to be averaged out and details to be less well defined.

Comparison of the water velocity plots (Figures 23b and 23d) seems to again show an agreement in the velocity profiles, with key distinctive features being present in some form for both plots. Similarly, there are some discrepancies such as the apparent reduced velocity at the centre of the main channel, but this can be explained by the averaging effects of the lower resolution plot generated by SWE MacTVD. It is important also to note that in the SWE MacTVD plot there are localised regions of instability signified by spikes in velocity (red spots at around

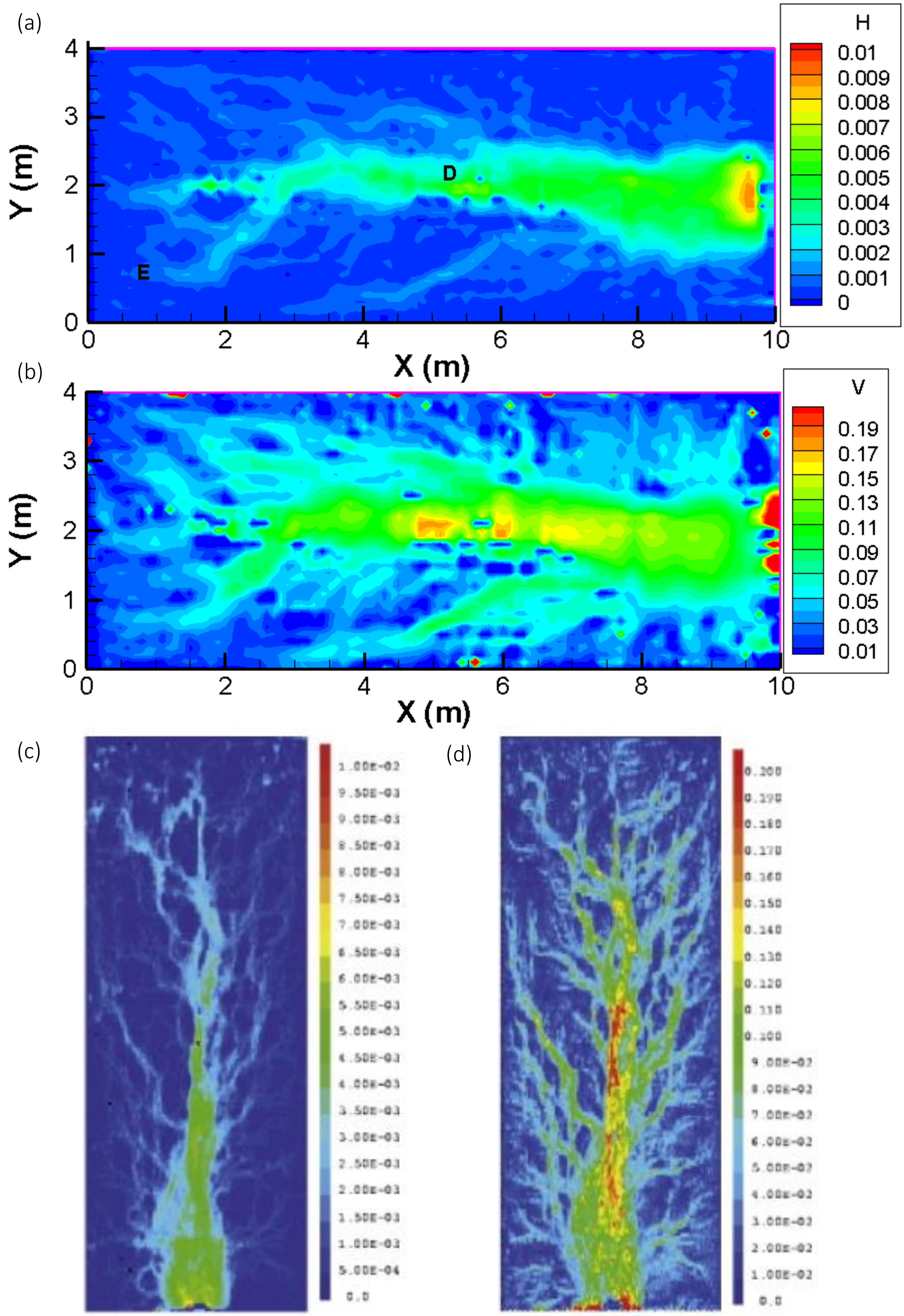

Figure 23 - Plan plots from SWE MacTVD of (a) water depth and (b) velocity as compared to plan plots from Mügler et al. of (c) water depth and (d) velocity

(5.6,0.1), (9.6,3.7), (9.8,3.4), and sporadically along the topmost boundary). These may be signs of locations in the catchment where there is a sudden change in gradient, which as explained before leads to instability due to SWE MacTVD's inability to handle flows that are too thin. However, these localised instabilities do not seem to have affected the majority of the flow data.

A more quantifiable measure of the accuracy of SWE MacTVD for modelling the catchment flow velocity can be found using the experimental velocity data. As mentioned above, a number of measurement stations were situated across the catchment (show as blue crosses in Figure 24), against which values from the modelled velocity field can be extracted and compared.

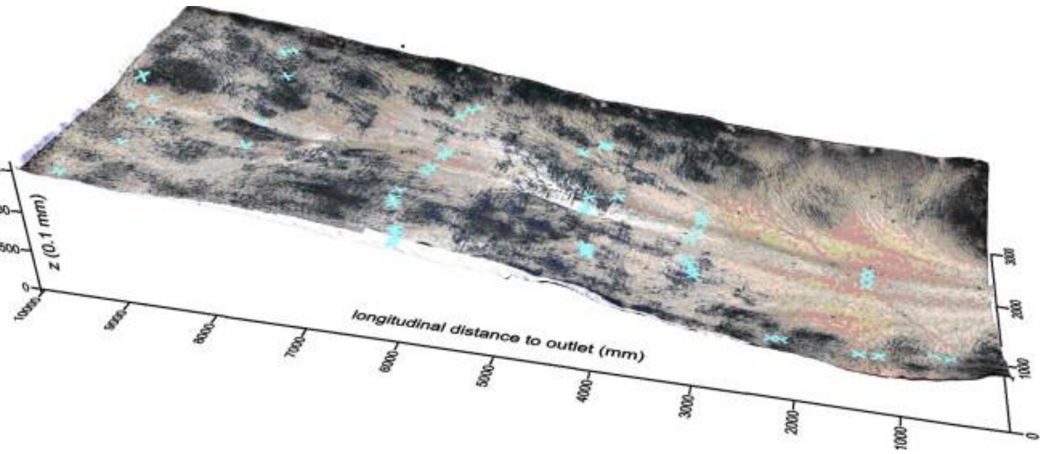

Figure 24 - Topography plot of Thies catchment with velocity measurement stations marked (Tatard, et al., 2008)

A plot of values of velocity at each station as measured in the SWE MacTVD model's plot against the velocity experimentally recorded is shown in Figure 25. The RMSE value of the plot as compared to direct proportionality is 0.03172 m/s. As well as this, visually, it is evident that there is a trend of agreement across the station velocities, with many of the points lying within a narrow band around proportionality.

It can be seen, however, that two of the points seem to deviate significantly from their expected values. These points are the only velocity values from the experimental data that are above 0.2 m/s. This may simply be due to experimental error, since these points seem to be anomalous as compared with the other velocity values.

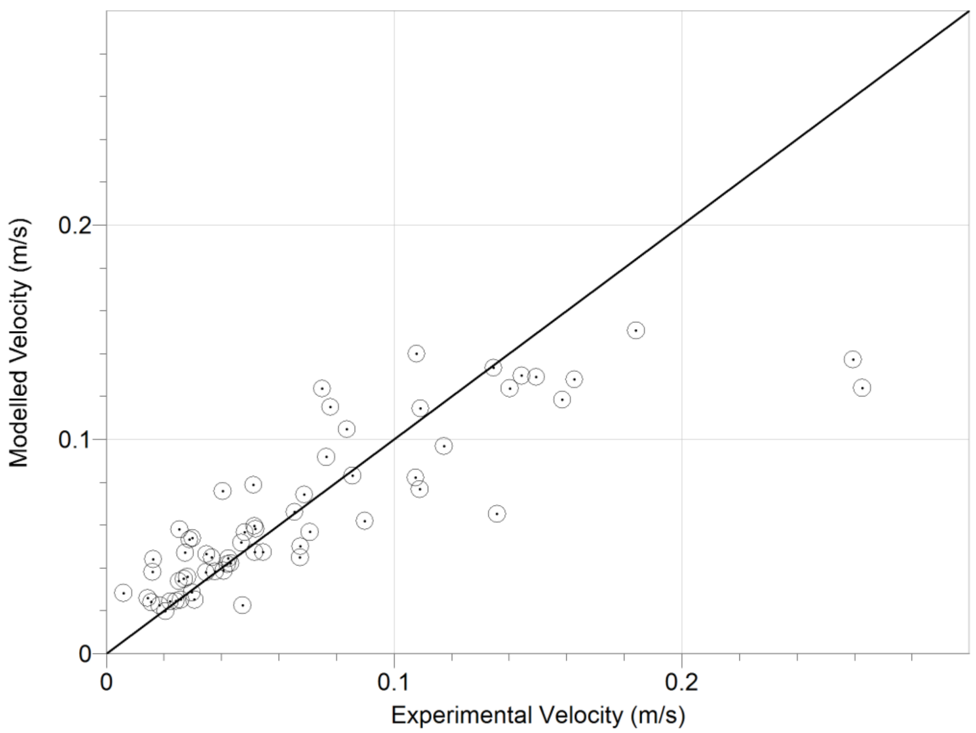

Figure 25 - Plot of velocity values calculated by SWE MacTVD against experimental velocity values

Mügler et al. performed a similar analysis using their constant Manning roughness simulation, the result of which is shown in Figure 26. Their simulation reached very similar solutions to that of SWE MacTVD, with most of the points lying in almost the same place. The RMSE value of their plot is 0.031 m/s. Their two anomalous points beyond 0.2 m/s measured velocity seem to corroborate the idea that their presence is not a sign of the failure of MacTVD: either they are anomalous points of raw data or there is a systematic error in the uniform roughness assumption causing higher velocities to not be adequately represented in the model.

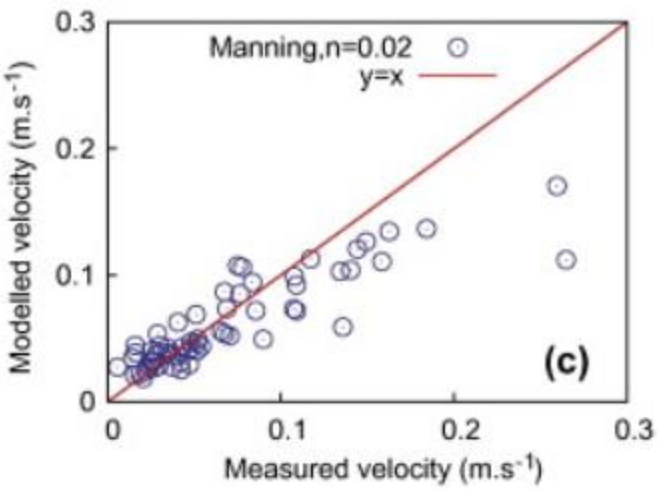

Figure 26 - Plot of velocity values calculated by Mügler et al. against experimental velocity values

Therefore, taking this into account, it can be concluded that, for this catchment, SWE MacTVD is an adequate model by which to derive velocity fields.

4.5.2 Validation of Solute Transport

With confirmation that the velocity field data is valid, the next step is to investigate whether the results generated by Solute MacTVD, using the velocity field data from SWE MacTVD, match with experimental data.

Of the 8 injection points in the original experiment, points D and E (shown relative to the topography in Figure 23a) were chosen to be used in this report as they are the only two upstream injection points that lie within the main channel, with E upstream of D.

Following on from Mügler et al.'s conclusions from their constant Manning roughness simulations, a roughness value of 0.018 was chosen as an accurate representation of the effective uniform roughness of the flows relating to points D and E. An example of the time progression of concentration over time for point D can be found in Figure 27, which shows the concentration of solute at various times after the initial release of pollutant.

After 5 seconds, Figure 27a, the pollutant is still localised to the source as well as a small region downstream of it. The fluid carries the pollutant around the small obstruction in the centre of the channel, shown by how the concentration cloud follows the velocity field and begins to envelop the obstruction.

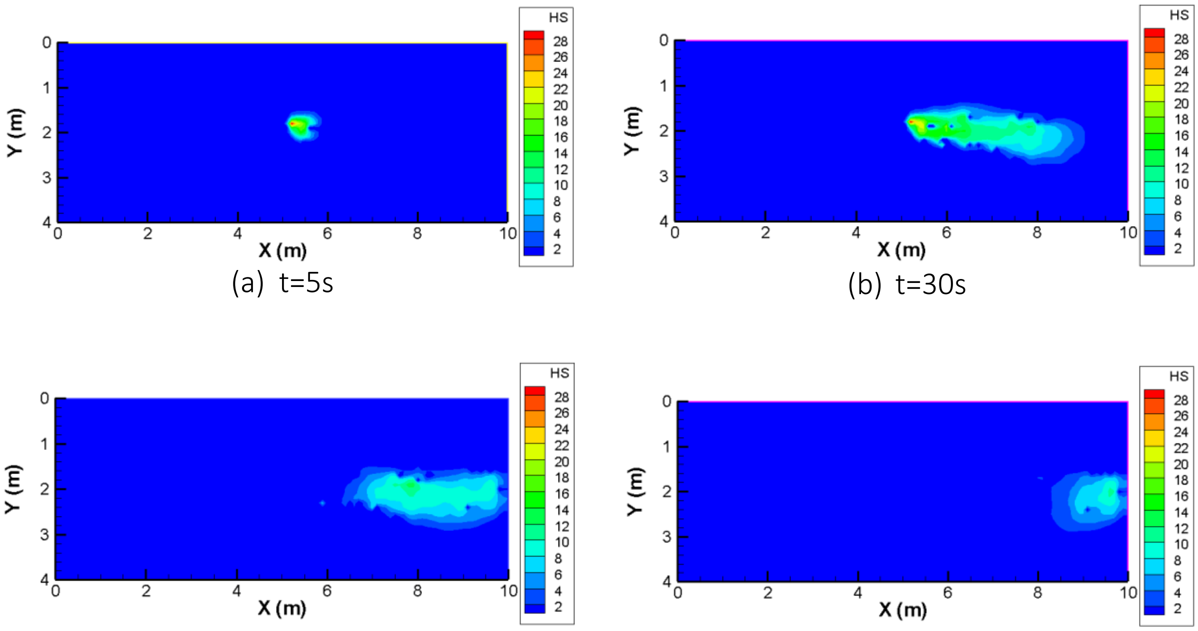

(a) t=5s (b) t=30s

(c) t=45s (d) t=60s

Figure 27 - Plot of HS distribution at (a) t=5s (b) t=30s (c) t=45s (d) t=60s

After 30 seconds, Figure 27b, just before the source contribution ceases, the concentration cloud has expanded further downstream, continuing to follow the velocity field.

After 45 seconds, Figure 27c, the concentration cloud has reached the outlet. Since it is past the 30s window where the source is active, solute lost from the catchment in outflow isn't being replaced, hence the concentration cloud receding from the location of the source.

After 60 seconds, Figure 27d, the solute continues to exit via the outflow without being replaced, and so the concentration cloud shifts gradually towards the outlet until all of the pollutant has passed through the catchment completely.

The output of Solute MacTVD can be easily manipulated give a non-depth averaged concentration at the outlet: the values of HS at the outlet boundary can be multiplied by H and then integrated along the boundary to obtain a value for the concentration of solute at a given time in the outflow of the catchment. This can then be converted to a conductivity value for comparison with experimental data based on the following linear relationship (12) (Mügler, *email correspondence*, 2014):

$$[\mathrm{Cl}^-]\ (\mathrm{mmol/L}) = (0.0141 \times \mathrm{Conductivity}\ (\mu\mathrm{S/cm})) - 5.1087 \qquad (12)$$

Plots showing conductivity over time for experimental data and data calculated from modelled concentrations at injection points D and E are shown in Figure 28.

Looking at Figure 28a and comparing the modelled and experimental conductance curves for point D, Solute MacTVD generates results that match experimental data fairly well. Both curves peak at around 55s and the widths of the peaks are similar such that the time period over which the conductivity signals are non-negligible are largely the same. There are three minor discrepancies that are visible.

Firstly, while the timing of the rise and fall of the modelled curve is similar enough to the experimental curve to be reasonably accurate, there is still a small offset of approximately 5s on the limbs of the curve itself due to a skew in the experimental data. This lies beyond the 1s time uncertainty acknowledged as a result of time synchronisation (Mügler, et al., 2011). Therefore, it could be considered that perhaps the effective of the roughness of the catchment for flows from point D is lower than 0.018, such that pollutant can travel to the outflow sooner by 5s.

Secondly, the general shapes of the curves, as alluded to above by the skewness, do not match. The modelled curve is near symmetric whereas the experimental curve is skewed, with the rising limb being less steep than the falling limb. This would not be expected if the

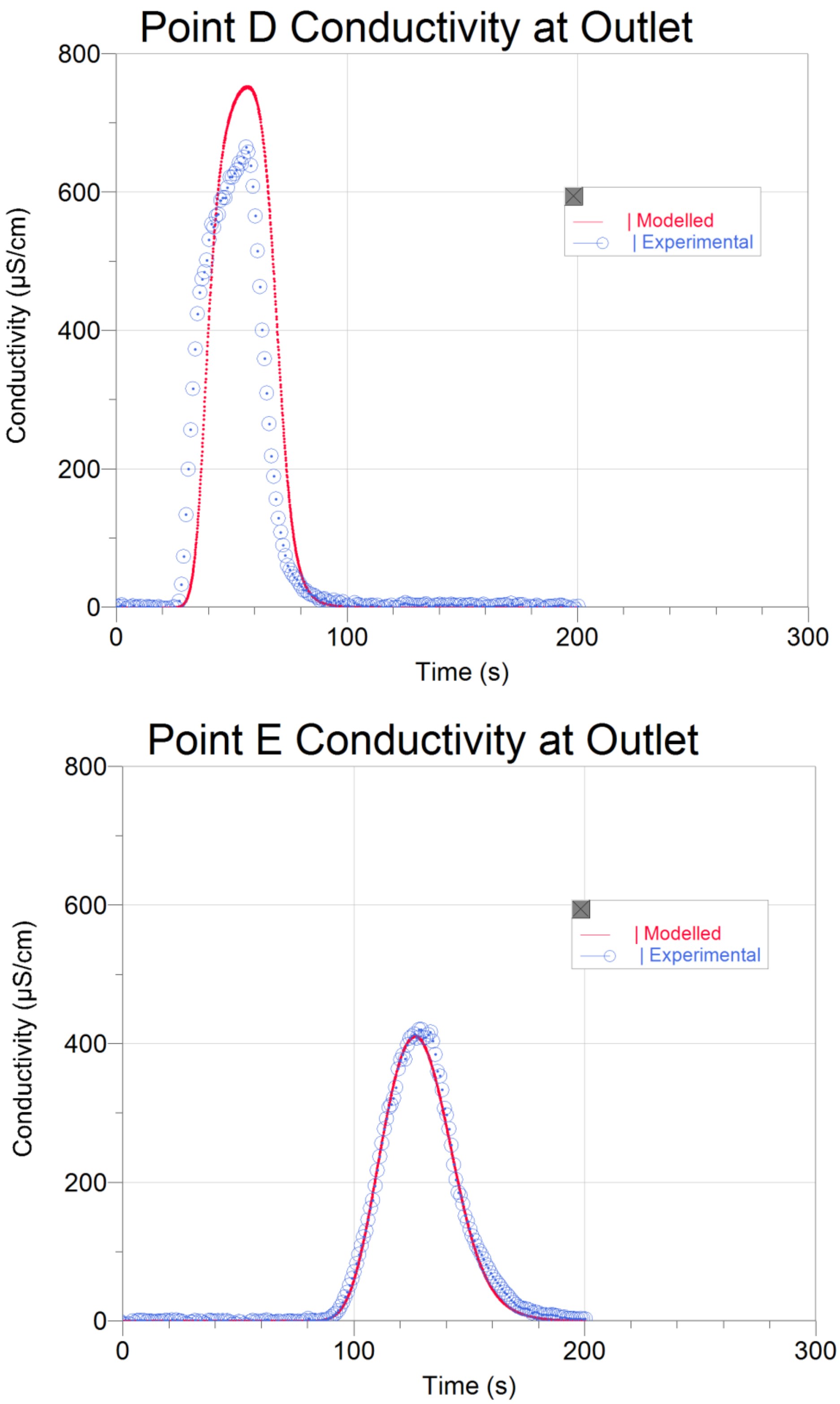

Figure 28 - Conductivity plot over time at outlet for tracer injection at (a) point D and (b) point E calculated by Solute MacTVD

solute follows, the velocity field exactly, as is assumed in the model. Therefore, it is possible there were, for example, areas of turbulence or temporary storage in the catchment such that an asymmetric conductance curve is created.

Finally, the magnitude of the peak of the modelled curve is greater than that of the experimental curve, with a modelled value of 755 µS/cm as opposed to the experimental peak of 665 µS/cm. This seems to suggest that less solute is making it to the outlet in the real-world: while the magnitude is lower, the width of the peak is the same and so there is less quantity of solute being observed experimentally. Perhaps this could be caused by solute being retained by surface storage in the catchment, or through the solute filtering into the ground before getting to the outlet.

Looking at Figure 28b and comparing the modelled and experimental conductance curves for point E, the two curves are nearly identical in terms of timing, shape and size: they both peak at around 125s to a conductivity around 420 µS/cm, and they are both relatively symmetric. This suggests that a roughness of 0.018 is a good match for modelling the flows from point E.

The one discrepancy that can be seen is that the modelled curve is approximately 1s ahead of the experimental curve, which is most visible in the falling limb of the curve. However, as previously mentioned, this 1s error is accounted for by the uncertainty of the measurement method.

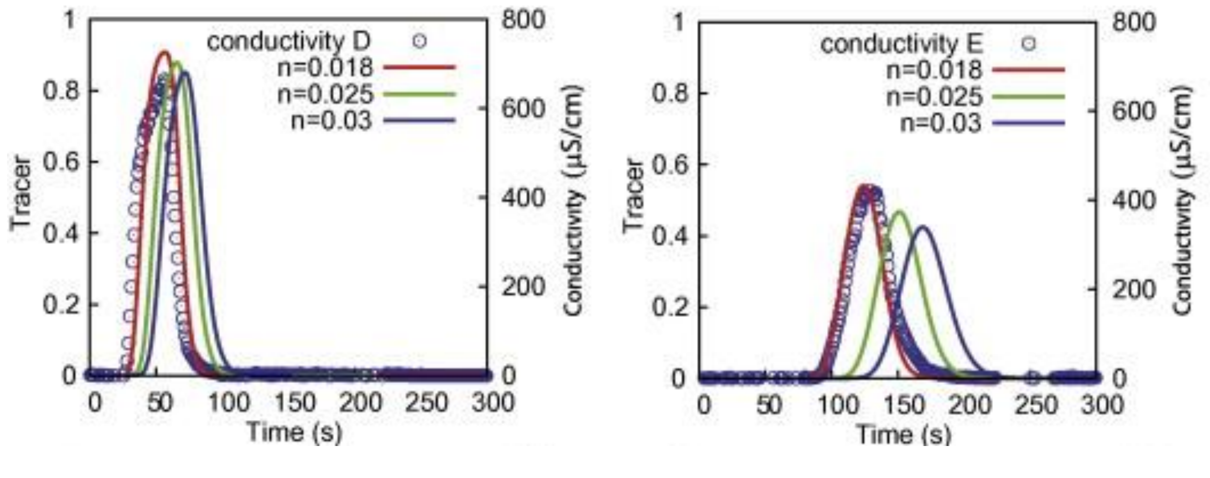

Figure 29 - Conductivity plot over time at outlet for tracer injection at (a) point D and (b) point E calculated by Mügler et al. (Mügler, et al., 2011)

Similar comparisons between experimental and simulated results were made by Mügler et al, the results of which are shown in Figure 29.

Comparison of Figure 28a and Figure 29a suggests that Solute MacTVD is not at fault for the discrepancies between the curves: the simulated results for a Manning roughness of 0.018 are also time-offset, symmetric, and of greater magnitude. In fact, the curves for the modelled and simulated cases match very well. Comparison of Figure 28b and Figure 29b further supports the idea that the modelled and simulated cases match, with both curves having the same characteristics down to the slight lead in the falling limb.

Overall, the close matching of the Solute MacTVD results to experimental values, as well as exact matching to the simulations of Mügler et al. indicating that deviations from experimental values are systematic, suggests that MacTVD is a viable model in this case.

4.6 Catchment Roughness Effects

The effect of changing surface roughness on pollutant transport was tested, making use of the Thies catchment for which MacTVD had been validated. Utilising the same topography but changing the constant value of Manning roughness allows comparisons to be made between the base case as validated above and cases where the roughness had been increased and decreased.

For both point D and E, further solutions for Manning roughness of 0.01 and 0.03 were obtained in order to contrast with the validation case with Manning roughness 0.018. The process involved recalculating the velocity field of the catchment using SWE MacTVD, and then applying that new velocity field with the new roughness to Solute MacTVD. The outlet conductivity was then obtained as before by integrating at the outlet boundary.

4.6.1 Mid-Field Release

Looking at Figure 30 and comparing the case where Manning roughness is 0.01 with the base case where Manning roughness is 0.018, it can be seen that the peak of the former occurs 10s earlier and reaches a maximum conductivity that is 38 μS/cm greater. Similarly, comparing the case where Manning roughness is 0.03 with the base case where Manning roughness is 0.018, it can be seen that the peak of the former occurs 16s later and reaches a maximum conductivity that is 60 μS/cm lower.

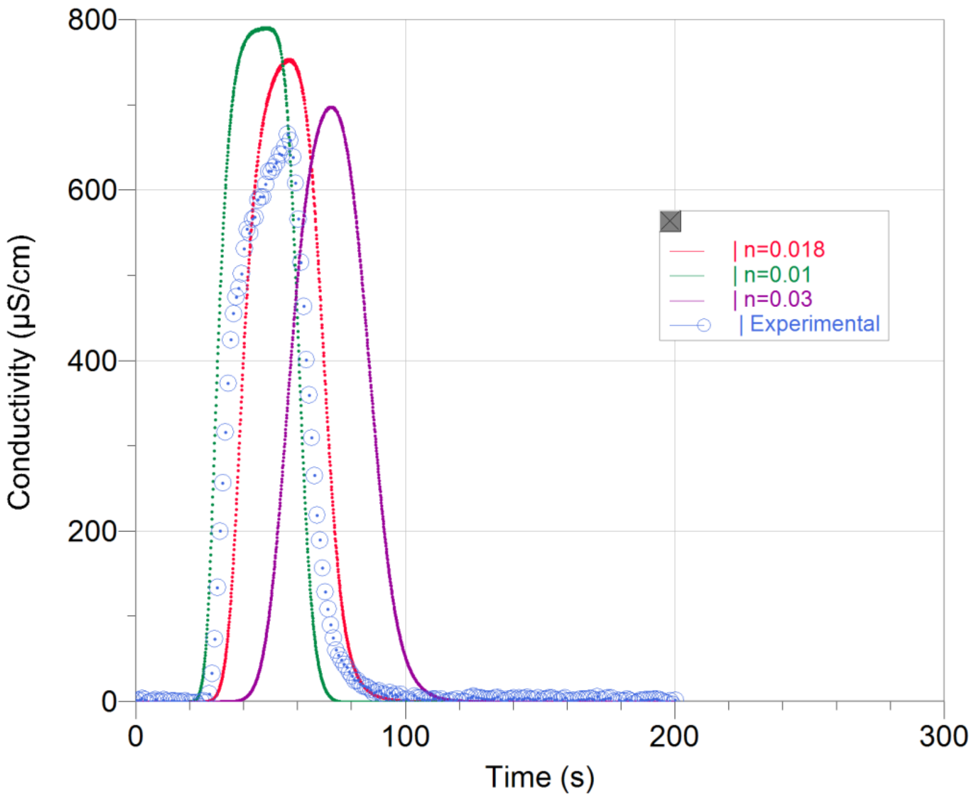

Figure 30 - Catchment roughness effects conductivity plots for tracer injection at point D for a range of roughness values calculated by Solute MacTVD

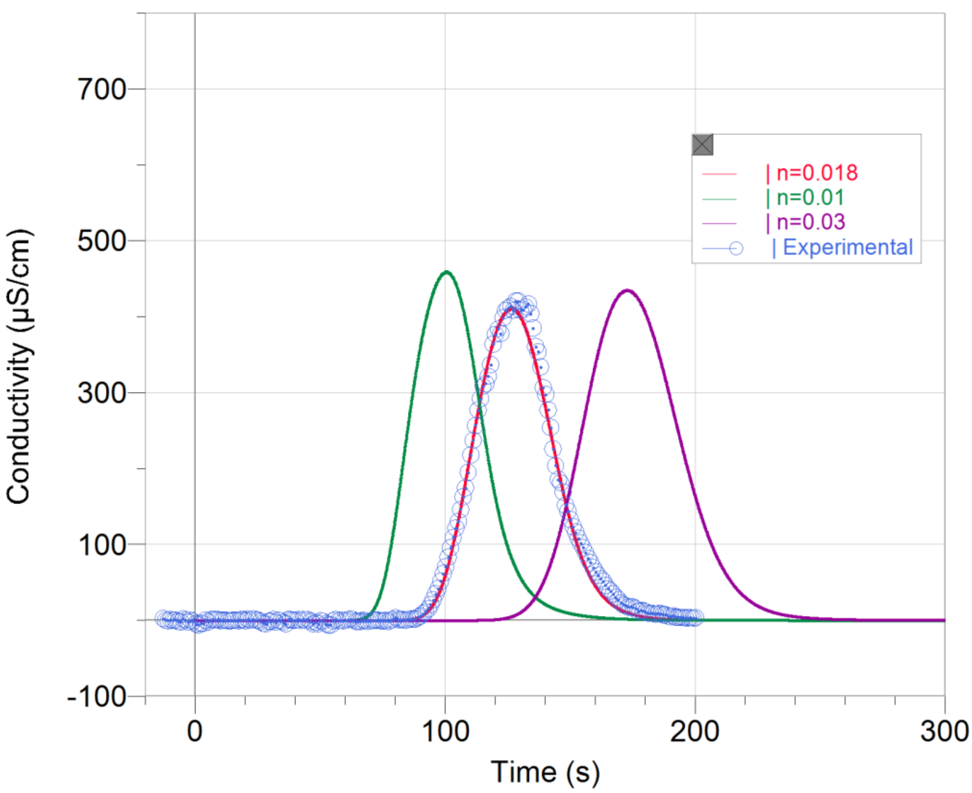

Figure 31 - Catchment roughness effects conductivity plots for tracer injection at point E for a range of roughness values calculated by Solute MacTVD

A potential explanation for these values is that as roughness increases, the velocity of the flow decreases, and therefore the solute is carried by the water more slowly (hence the later arrival times) and more spread out (hence the lower peaks).

4.6.2 Upstream Release

Looking at Figure 31 and comparing the case where Manning roughness is 0.01 with the base case where Manning roughness is 0.018, it can be seen that the peak of the former occurs 26s earlier and reaches a maximum conductivity that is 42 μS/cm greater. On the other hand, comparing the case where Manning roughness is 0.03 with the base case where Manning roughness is 0.018, it can be seen that the peak of the former occurs 47s later but reaches a maximum conductivity that is 17 μS/cm greater.

This last result is unexpected since the trend from point D would suggest that the peak for the 0.03 Manning roughness case should be lower. This result will later be examined with reference to Mügler et al.'s results.

4.6.3 Summary

The overall trend observed across both points is that the higher the roughness of the catchment, the longer it takes for pollutant to travel to the outlet. Furthermore, aside from the result for point E at roughness 0.03, it appears there is also a trend that the higher the roughness, the lower the peak conductivity and hence concentration.

4.7 Comparison to Mügler et al

In the paper by Mügler et al. (Mügler, et al., 2011), some experimentation was performed to determine the best value for Manning roughness to uniformly apply to the catchment in order to best lead to a solution comparable to experimental results. Some of these results at different roughness values can be used to compare with the catchment roughness results obtained. The relevant curves can be found in Figure 29, where roughness values of 0.018 and 0.03 are shown.

For point D, the simulated curve of Manning roughness 0.03 agrees with the MacTVD result, with an identical time delay and a maximum conductivity of equal (marginally smaller) magnitude.

For point E, the simulated curve of Manning roughness 0.03 does not agree with the MacTVD result. While the time delay again agrees, the magnitude of the peak of the simulated curve is much lower than that obtained using MacTVD.

While for point D, the simulation results from Mügler et al. corroborate the trends observed by the MacTVD model, for point E they do not, specifically regarding the magnitude of the peak for the curve of 0.03 Manning roughness. Given that the simulated version of this curve agrees with the trend outline by point D, it is possible that the Solute MacTVD value is erroneous.

5 Conclusions

This report set out to investigate the effects of roughness and macro-roughness on flow fields in the context of NFM techniques using SWE MacTVD, and of catchment roughness on pollutant transport using Solute MacTVD. This was motivated by the wish to learn more about the impact of rewilding as a countermeasure to the big issues of surface runoff flash flooding and nitrate pollution.

To start with, while setting up the model, it was noted there are some limitations to MacTVD. Firstly, SWE MacTVD does not by default assume a free boundary condition and therefore an adjustment must be made beyond the outlet by adding an extension if such a condition is required. Secondly, a free boundary is still not possible because the numerical nature of the model means a minimum depth exists below which the calculations become unstable, limiting the degree to which catchment geometry can be formed.

Once set up, SWE MacTVD was validated for several uniform slope test cases. Comparison of the SWE MacTVD calculated solution to the 1D uniform roughness slope detailed by Gottardi & Venutelli with experimental and numerical results yielded a strong correlation between the SWE MacTVD model and previous data, with deviations from experimental values explainable by real-world effects that were too nuanced to be accounted for in the model. Comparison with varied roughness slope solutions by Huang & Lee yielded equally consistent results for both 100min and 30 min rainfall events, with only a small deviation in the peak discharge for the 30min event, which can be accounted for by the fact that SWE MacTVD cannot perfectly replicate the outlet boundary condition.

The 1D roughness strip experiment showed the effect of changing a strip of surface roughness on a catchment's discharge. It was found that after the rainfall downstream of the strip had flowed out, there was a lag period cause by the roughness strip before the curve resumed. There was a similar lag period in the falling limb of the curve. It was noted that as the roughness of the strip increased, the maximum discharge decreased, and the time of concentration increased. There were diminishing returns for the impact of increasing roughness on reducing peak discharge, and to a lesser extent on increasing time of concentration.

Investigating macro-roughness showed the impact of larger or more frequent irregularities in the surface of a catchment. Increasing magnitude in a periodic macro-roughness slope reduces the maximum runoff and prolongs the time of concentration, but the scope of the analysis was limited by numerical stability of the model. Increasing the magnitude could be seen as analogous to increasing the effective roughness. Changing the frequency of such a catchment macro-roughness allowed an optimum frequency coefficient of around $0.55m^{-1}$ to be found for this particular case. Frequencies lower than this tend towards a flat slope and frequencies higher than this cause gradients that allow runoff to escape the trapping effect.

SWE MacTVD and Solute MacTVD were then validated against the velocity and transport modelling data of the Thies catchment respectively. SWE MacTVD generated plots very similar to simulations run by Mügler et al. and comparison with experimental data showed a strong correlation to proportionality between SWE MacTVD-modelled and experimental velocities. Application of this velocity data to Solute MacTVD generated a convincing evolution of concentration contours for both injection points D and E. Comparison of Solute MacTVD solutions with experimental and simulated data showed good correlation.

The catchment roughness was then altered to investigate the impact of roughness on pollutant transport. The overall trend observed across both points was that the higher the roughness of the catchment, the longer it took for pollutant to travel to the outlet. Furthermore, aside from the result for point E at roughness 0.03, it appeared as though there was also a trend that the higher the roughness, the lower the peak concentration. These catchment roughness results were then compared with simulation data from Mügler et al. All data was in agreement aside from the result for point E at roughness 0.03, whose validity could be called into question, considering that the simulated data conforms with the hypothesised trend.

Further research that could be undertaken could include:

- An examination of rewilding strip area/location for a uniform slope case
- Different functions/slopes/roughnesses for the macro-roughness experiment
- A wider range of transport catchment roughness values/testing of roughness strips

Overall, this report successfully investigated its aims and has come to useful conclusions about surface runoff and pollutant transport.

6 References

BBC News. (2019, Nov 8). *Sheffield flooding: Torrential rain leaves city flooded*. Retrieved from BBC News: https://www.bbc.co.uk/news/uk-england-50333233

Burguet, M., Guzmán, G., de Luna, E., Taguas, E., & Gómez, J. (2018). Evaluation of disruption of sediment connectivity and herbicide transport across a slope by grass strips using a magnetic iron oxide tracer. *Soil and Tillage Research, 180*, 268-281.

Busby, M. (2019, Dec 27). *UK weather: floods close Devon roads as groundwater levels rise*. Retrieved from The Guardian: https://www.theguardian.com/uk-news/2019/dec/27/uk-weather-flood-warnings-remain-in-place-across-england

Carver, S. (2016, Sep 8). *Stem the floods – don't hold back rewilding*. Retrieved from Rewilding Britain: https://www.rewildingbritain.org.uk/blog/dont-hold-back-rewilding

Cea, L., Garrido, M., & Puertas, J. (2008). Hyrdrological forecasting of fast flood events in small catchments with a 2D-SWE model. Numerical model and experimental validation. *World Water Congress 2008.* Montpellier.

Cea, L., Garrido, M., & Puertas, J. (2010). Experimental validation of two-dimensional depth-averaged models for forecasting rainfall–runoff from precipitation data in urban areas. *Journal of Hydrology, 382*(1), 88-102.

Chan, Y. (2012). *Rainfall-runoff processes in urban environments.*

Collins, A., Stutter, M., & Kronvang, B. (2014). Mitigating diffuse pollution from agriculture: International approaches and experience. *Science of The Total Environment, 468-469*, 1173-1177.

Davies, G. (2019, Nov 11). *UK weather: Residents of flooded village complain they weren't warned of risk, as further heavy rain forecast* . Retrieved from The Telegraph: https://www.telegraph.co.uk/news/2019/11/11/uk-weather-residents-flooded-village-complain-werent-warned/

Davis, A., Stagge, J., Jamil, E., & Kim, H. (2012). Hydraulic performance of grass swales for managing highway runoff. *Water Research, 46*(20), 6775-6786.

Dong, W., Wang, Q., Zhou, B., & Shan, Y. (2013). A simple model for the transport of soil-dissolved chemicals in runoff by raindrops. *CATENA, 101*, 129-135.

Ferreira, C., Moruzzi, R., Isidoro, J., Tudor, M., Vargas, M., Ferreira, A., & de Lima, J. (2019, 12). Impacts of distinct spatial arrangements of impervious surfaces on runoff and sediment fluxes from laboratory experiments. *Anthropocene, 28*, 100219.

Gan, F., He, B., & Qin, Z. (2020). Hydrological response and soil detachment rate from dip/anti-dip slopes as a function of rock strata dip in karst valley revealed by rainfall simulations. *Journal of Hydrology, 581*, 124416.

Gao, B., Walter, M., Steenhuis, T., Parlange, J.-Y., Richards, B., Hogarth, W., & Rose, C. (2005). Investigating raindrop effects on transport of sediment and non-sorbed chemicals from soil to surface runoff. *Journal of Hydrology, 308*(1), 313-320.

Gottardi, G., & Venutelli, M. (2008). An accurate time integration method for simplified overland flow models. *Advances in Water Resources, 31*(1), 173-180.

Havis, R., Smith, R., & Adrian, D. (1992). Partitioning solute transport between infiltration and overland flow under rainfall. *Water Resources Research, 28*(10), 2569-2580.

Hou, J., Guo, K., Liu, F., Han, H., Liang, Q., Tong, Y., & Li, P. (2018, 9 15). Assessing Slope Forest Effect on Flood Process Caused by a Short-Duration Storm in a Small Catchment. *Water, 10*(9), 1256.

Huang, J., & Lee, K. (2009). Influences of spatially heterogeneous roughness on flow hydrographs. *Advances in Water Resources*.

Huang, J., Xu, C.-c., Ridoutt, B., Wang, X.-c., & Ren, P.-a. (2017). Nitrogen and phosphorus losses and eutrophication potential associated with fertilizer application to cropland in China. *Journal of Cleaner Production, 159*, 171-179.

Lamb, K., MacQuarrie, K., Butler, K., Danielescu, S., Mott, E., Grimmet, M., & Zebarth, B. (2019). Hydrogeophysical monitoring reveals primarily vertical movement of an applied tracer across a shallow, sloping low-permeability till interface: Implications for agricultural nitrate transport. *Journal of Hydrology, 573*, 616-630.

Lehman, O., & Ahuja, L. (1985). Interflow of water and tracer chemical on sloping field plots with exposed seepage faces. *Journal of Hydrology, 76*(3), 307-317.

Leroy, M.-c., Portet-Koltalo, F., Legras, M., Lederf, F., Moncond'huy, V., Polaert, I., & Marcotte, S. (2016). Performance of vegetated swales for improving road runoff quality in a moderate traffic urban area. *Science of The Total Environment, 566-567*, 113-121.

Liang, D., Falconer, R., & Lin, B. (2006). Comparison between TVD-MacCormack and ADI-type solvers of the shallow water equations. *Advances in Water Resources*, 1833-1845.

Liang, D., Lin, B., & Falconer, R. (2007, 2 20). Simulation of rapidly varying flow using an efficient TVD-MacCormack scheme. *International Journal for Numerical Methods in Fluids, 53*(5), 811-826.

Liang, D., Wang, X., Falconer, R., & Bockelmann-Evans, B. (2010). Solving the depth-integrated solute transport equation with a TVD-MacCormack scheme. *Environmental Modelling & Software, 25*(12), 1619-1629.

Maske, S., & Jain, M. (2014, 2 15). Study on effect of surface roughness on overland flow from different geometric surfaces through numerical simulation. *Hydrological Processes, 28*(4), 2595-2616.

Mügler, C., Planchon, O., Patin, J., Weill, S., Silvera, N., Richard, P., & Mouche, E. (2011). Comparison of roughness models to simulate overland flow and tracer transport experiments under simulated rainfall at plot scale. *Journal of Hydrology*.

Nestler, A., Berglund, M., Accoe, F., Duta, S., Xue, D., Boeckx, P., & Taylor, P. (2011). Isotopes for improved management of nitrate pollution in aqueous resources: Review of surface water field studies. *Environmental Science and Pollution Research, 18*(4), 519-533.

Pidcock, R. (2014). *How much flooding is in the UK's future? A look at the IPCC report.* Retrieved Nov 21, 2019, from CarbonBrief: https://www.carbonbrief.org/how-much-flooding-is-in-the-uks-future-a-look-at-the-ipcc-report

Rujner, H., Leonhardt, G., Marsalek, J., & Viklander, M. (2018). High-resolution modelling of the grass swale response to runoff inflows with Mike SHE. *Journal of Hydrology, 562*, 411-422.

Semmens, D., Goodrich, D., Unkrich, C., Smith, R., Woolhiser, D., & Miller, S. (2007, 1 1). KINEROS2 and the AGWA modelling framework. *Hydrological Modelling in Arid and Semi-Arid Areas*.

SEPA. (2015). *Natural Flood Management Handbook.*

Sky News. (2019, Nov 23). *UK weather: Two inches of rain and flooding expected in parts of UK*. Retrieved from Sky News: https://news.sky.com/story/uk-weather-flood-hit-parts-of-britain-facing-weekend-downpours-and-theyre-not-the-only-ones-11867298

Susdrain. (2020). *Component: Swales*. Retrieved from Susdrain: https://www.susdrain.org/delivering-suds/using-suds/suds-components/swales-and-conveyance-channels/swales.html

Tatard, L., Planchon, O., Wainwright, J., Nord, G., Favis-Mortlock, D., Silvera, N., . . . Huang, C. (2008). Measurement and modelling of high-resolution flow-velocity data under simulated rainfall on a low-slope sandy soil. *Journal of Hydrology, 348*(1), 1-12.

Wallace, C. (2019). *Simulations of Rainfall-Runoff Processes and the Effectiveness of Natural Flood Management Schemes.*

Walton, R., Volker, R., Bristow, K., & Smettem, K. (2000). Experimental examination of solute transport by surface runoff from low-angle slopes. *Journal of Hydrology, 233*(1), 19-36.

Wong, T., & Li, Y. (1998). *Theoretical assessment of changes in design ¯ood peak of an overland plane for two opposing urbanization sequences.*

Wu, Y., Woolhiser, D., & Yevjevich, V. (1982). Effects of spatial variability of hydraulic resistance of runoff hydrographs. *Journal of Hydrology*.

Xiao, Y., Zhang, T., Liang, D., & Chen, J. (2016). Experimental study of water and dissolved pollutant runoffs on impervious surfaces. *Journal of Hydrodynamics*.

Yan, Y., Dai, Q., Yuan, Y., Peng, X., Zhao, L., & Yang, J. (2018). Effects of rainfall intensity on runoff and sediment yields on bare slopes in a karst area, SW China. *Geoderma, 330*, 30-40.

A) Symbol Definitions

Symbol	Units	Definition
β	-	Correction factor for non-uniform vertical velocity (=1 for uniform)
η	m	Water surface elevation above datum
t	s	Time
q_x	m^2/s	Discharge per unit width in the x direction
q_y	m^2/s	Discharge per unit width in the y direction
g	m/s^2	Gravitational acceleration
H	m	Total water column depth
C	$m^{0.5}/s$	Chezy bed roughness coefficient
Δt	s	Time step
Δx	m	Cell length
v	m/s	Characteristic velocity
C_0	-	Courant number (=1 for explicit schemes)
S	kg/m^2	Depth averaged concentration of solute
U	m/s	Velocity component in x direction
V	m/s	Velocity component in y direction
q_s	kg/ms	Source/Sink contribution per unit area
ε_l	-	Longitudinal dispersion constant
ε_t	-	Turbulent diffusion constant

B) Risk Assessment Retrospective

The main risk with computer-based work, especially with the processing of large amount of data, is the risk of eye strain if the screen is stared at too long. This was remedied by looking away from the screen about every half an hour to ensure eye strain was mitigated.

As well as this, bad posture or seating position can cause body aches and pains. This issue was minimised by following recommended guidelines for computing working environment setups. Also, staying seated at the computer for long durations can equally cause body pain, which was mitigated by getting up and moving around frequently before pain occurred.

Finally, another risk of handling a large amount of data is that of repetitive strain injury from repeated data processing movements with the mouse. This was mitigated by ensuring the mouse arm was in the proper position and that breaks were taken long before the fingers or hands started to tire.

Overall, these risks are easily overlooked and can have lasting impact on health, so care should be taken in the future to continue to follow the guidelines.